AN ABSTRACT OF THE THESIS OF

Seog-Young Han for the degree of Doctor of Philosophy in Mechanical Engineering presented on January 31, 1989.

Title: Elastodynamic Analysis of a Propagating Finite Crack in a Micropolar Elastic Solid

Abstract approved: Redacted for Privacy
Timothy C./Kennedy

Redacted for Privacy
Mysore N. L. Narasimhan

A dynamic propagation of a finite crack of opening mode in a micropolar elastic solid was investigated. By using an integral transform method, a pair of two-dimensional singular integral equations governing stress and couple stress was formulated in terms of the displacement transverse to the crack, macro- and micro-rotations, and microinertia. These integral equations are solved numerically. Solutions for dynamic stress intensity and couple stress intensity factors are obtained by utilizing the values of the strengths of the square root singularities in the macro-rotation and the gradient of the micro-rotation at the crack tips. The

motion of the crack tips and the load on the crack surface are not prescribed in the formulation of the problem. Therefore, the method of solution is applicable to nonuniform rates of propagation of a crack under an arbitrary time-dependent load on the crack surface. The behavior of the micro-rotation field, and the dynamic couple stress intensity factor, which are influenced by microinertia, in addition to the dynamic stress intensity factor, are examined. The classical elasticity solution for the corresponding problem follows as a special case of our solution when the micropolar moduli are dropped.

Elastodynamic Analysis of a Propagating Finite Crack in a Micropolar Elastic Solid

by

Seog-Young Han

A THESIS

submitted to

Oregon State University

in partial fulfillment of
the requirements for the
degree of

Doctor of Philosophy

Completed January 31, 1989

Commencement June 1989

APPROVED:

Redacted for Privacy

Associate Professor of Mechanical Engineering in Charge of Major

Redacted for Privacy

Professor of Mathematics in Charge of co-field

Redacted for Privacy

Head of Department of Mechanical Engineering

Redacted for Privacy

Dean of Graduate School

Date thesis is presented January 31, 1989

Typed by B. McMechan for Seog-Young Han

ACKNOWLEGEMENT

I would like to express my appreciation to Dr. Timothy C. Kennedy and Dr. Mysore N. L. Narasimhan for their valuable advice and kindness. Dr. Kennedy helped me with the concept of fracture mechanics, and Dr. Narasimhan assisted me with the concept of dynamic fracture mechanics, as well as the techniques of research analysis. I was very fortunate to have two knowledgeable, kind and helpful advisors. I would also like to express my appreciation to Dr. Charles E. Smith, Dr. Alan H. Robinson and Dr. Martin L. Hellickson for serving as my doctoral committee members.

I would also like to express my appreciation to my parents for their endless love and encouragement, and thanks to my wife, Kyoung-Sook, and my son, Tak-Jin, for their love and patient endurance.

Table of Contents

List of Figures

ELASTODYNAMIC ANALYSIS OF A PROPAGATING FINITE CRACK IN A MICROPOLAR ELASTIC SOLID

CHAPTER 1

INTRODUCTION

1.1 General Remarks

The classical theory of elasticity is based on the fundamental assumptions that all material bodies possess continuous mass densities, all balance laws are valid for every part of the body no matter how small it may be, and the state of the body at any material point is influenced only by the infinitesimal neighborhood about that point. These assumptions lead to a description of the deformation of the body in terms of the symmetric strain and stress tensors. In fact, the first of the assumptions means the atomic, pore and grain structure of real materials is to be disregarded. It is also proved to be an untenable assumption by the fact that molecular theories and atomistic models of the materials have shown that mass density can be markedly different from the assumed continuous mass density when the size of the volume element is below a certain

limit value. The second of the assumptions eliminates the long-range effect of loads on the motion and the evolution of the state of the body. The third assumption ignores the effect of long-range interatomic interactions.

The results, derived on the basis of classical elasticity, are in good agreement with experiments performed on numerous structural materials below the elasticity limit of the material. However, in many cases essential differences have been observed between theory and experiment; this fact refers first of all to the states of stress in which there occur large stress gradients. As an example of such a state one may mention the stress concentration in the vicinity of holes, or near notches and cracks. The discrepancy between classical elasticity and experiment becomes particularly important in problems of dynamics, namely in the case of elastic vibrations characterized by large frequencies and small wavelengths; that is, for example, in the case of ultrasonic waves. The discrepancy is due partly to the fact that in the case of large frequencies and small wavelengths, the microstructure of the body becomes important. Classical elasticity fails to produce good results in the case of vibrations of granular bodies with large molecules, such as polymers. A possible explanation is that the constitutive equation of classical theory may not be sufficiently general.

In order to eliminate these shortcomings of classical elasticity, several generalized continuum theories have been introduced which have additional degrees of freedom. The most widely accepted of these are the couple stress theory (indeterminate couple stress theory) introduced by Mindlin and Tiersten [1] and others, and the micropolar continuum theory introduced and developed by Eringen and Suhubi [2]. The couple stress theory arises as a special case of the micropolar elasticity under certain restrictions.

A microcontinuum is a continuous medium to each point of which is assigned another sub-continuum, this latter being able to translate, rotate and deform. The micropolar medium is a special case of the microcontinuum with the property that the sub-continuum defined above can only translate and rotate without deforming even though the medium as a whole can translate, rotate and deform. The state of strain in a micropolar medium is described by two vectors, namely the displacement vector and the microrotation vector, and these vectors are connected with the stress tensor and the couple stress tensor. Central to the microcontinuum theories is the concept of couple stress. Materials wherein couple stresses and body couples are recognized to be acting are known as polar materials or oriented media. The existence and basis of couple stress in elasticity

was noted by Voigt [3] in connection with polar molecules in his work on crystallography. Duhem [4] postulated a theory that a body should be considered as an assemblage of not only points but also of directions associated with points.

E. and F. Cosserat [5] presented a unified theory for deformable bodies. A Cosserat continuum is defined as a three-dimensional continuum, each point of which is supplied with a triad of vectors called "directors" and which is amenable to a simple but elegant interpretation of the motion. The important monograph of the Cosserats [5] was buried in the literature nearly half a century until the topic was reopened and reconsidered in the 1950's. The idea of a Cosserat continuum was revived in various special forms by Günther [6], Grioli [7], Truesdell and Toupin [8], Aero and Kuvshinski [9], Schaefer [10], Mindlin and Tiersten [1], Toupin [11] and Eringen [12]. These early theories are mostly known as the "constrained theories" or the "indeterminate couple stress theory". Eringen and Suhubi [2] and Eringen [13] introduced a general theory of a nonlinear microelastic continuum in which the balance laws of classical continuum are supplemented with additional ones, and the intrinsic motions of microelements contained in a macrovolume element are taken into account. This theory, in special cases, contains the Cosserat continuum and the indeterminate couple stress theory.

In micropolar theory of elasticity, the strain and stress tensors are no longer symmetric. Thus, micropolar continuum theory has a mechanism which is capable of incorporating the internal long-range cohesive forces and yet remain within the basic continuum framework. A consequence of this feature is that the medium can support couple stress, spin and microinertia. The constitutive theory for micropolar media consists of a stress constitutive equation involving microrotation and a couple stress constitutive equation involving the gradients of microrotation. The field equations are augmented by a conservation law for microinertia. Since the axiom of locality is still used in micropolar continuum theory, it will not involve the effects of all the remaining material points of the body, which only the nonlocal continuum theory takes into account. However, the microcontinuum theory is also a nonlocal theory in the following sense. Eringen [14] has shown that the microcontinuum theory can be derived by defining suitable integral operators using certain test functions based on moment expansion techniques. These higher order moments incorporate to a certain extent the nonlocal interactions of microconstituents of the material. But, these moments have to be taken to indefinitely higher orders. The nonlocal theory, originated by Eringen [15], eliminates the need for taking such higher order moments and is designed to incorpor-

ate the interatomic interactions. New concepts of microinertia, spin momentum (intrinsic moment of momentum), body couple density and couple stress, which have no counterpart in classical theory of elasticity are brought out. The local balance laws of classical continuum theory are simply obtained by dropping the terms related to microvolume elements. Therefore, the micropolar continuum theory is a sophisticated continuum theory in which the local balance laws are supplemented with additional ones, and the important intrinsic motions of constituents (microvolume elements) contained in a macrovolume element are taken into account.

The micropolar theory of elasticity is relatively simple to use, and is versatile enough to find numerous important applications explaining many real physical phenomena. Materials with dumbbell molecules, liquid crystals, materials with elongated grains and composites which cannot be properly treated by classical elasticity, can be elegantly treated with the micropolar elasticity. The micropolar theory of elasticity is a powerful continuum theory to treat complex problems, including wave propagation and dispersion in solids, stress concentration around holes in bodies, and stress distribution at the crack tip of advancing line cracks in materials subject to external loads as well as boundary layers, turbulence, instabilities in

fluid flows, rotating fluids, and surface tension phenomena in fluids. Although there are several hundred papers in this and related fields, it still affords further exploration. Nevertheless, it seems that the logical foundation of the theory is solid and promising for the understanding of physical phenomena.

1.2 Scope of the Study

In dynamic crack propagation, conventional methods of solution are not easily applicable to finite crack problems for various reasons. For example, the Wiener-Hopf technique becomes very complicated as a result of the dynamic interaction of the crack tips in the case of a finite crack. Most of the works in dynamic crack propagation have dealt with semi-infinite crack problems which are tractable. As a result of lack of adequate tools of analysis, very little work has been done on dynamic finite crack problems even in classical theory of elasticity. To the best of our knowledge, there have been no investigations of dynamic crack propagation in micropolar elastic media.

The object of this study is to obtain the dynamic stress and the dynamic couple stress intensity factors for a finite crack whose tips may propagate nonuniformly in time under an arbitrary time dependent normal load on the crack surface. By using an integral trans-

form method, a pair of two-dimensional singular integral equations governing dynamic stress and dynamic couple stress is formulated. The analysis determines that both the macrorotation and the gradient of the microrotation of the crack surface can be determined by solving these singular integral equations. In addition, it is shown in this work that both the dynamic stress and the couple stress intensity factors can be obtained by utilizing the values of the strengths of the square root singularities in microrotation and the gradient of the microrotation at the crack tips. From this analysis, we have investigated the behavior of the microrotation field and the dynamic couple stress intensity factor, influenced by microinertia, which have not been considered in the classical theories of elasticity. The classical elasticity solution for the corresponding problem presents a special case when the micropolar moduli are dropped from the present solution.

1.3 Background of the Dynamic Fracture Investigations

During the past three decades, significant studies have been made in understanding fracture mechanics. These advances have encompassed both the fracture process itself and improved design criteria for engineering structures.

The majority of the past work on fractures has been devoted to the events which lead up to the onset

of crack propagation. However, it is equally important to be concerned with those process that govern the time-dependent motion or growth of cracks. In recent years, a substantial amount of work has been done in the area of dynamic fracture mechanics. Much of the work has been summarized in the review articles by Erdogan [16], Achenbach [17,18], Freund [19,20], Goel [21] and Williams and Knauss [22]. The literature in this area can be divided into three categories: steady-state problems, transient problems, and fully dynamic problems.

The first proper analysis of a moving crack is believed to have been done by Yoffe [23], who attempted to explain the branching of cracks by analyzing a dynamic steady-state problem in which a crack of fixed length travels at constant velocity under the influence of uniaxial tension. A similar steady-state problem was solved by Craggs [24] for a semi-infinite crack propagating at constant rate under the action of distributed loads on the crack surface which are fixed with respect to the crack tip. From the stress solutions in [23] and [24], it was found that the maximum stress $\sigma_{\theta\theta}$ moves out of the plane of crack propagation and acts at an angle of 60° to the direction of crack propagation when the crack velocity exceeds 0.6 times the shear wave velocity. Unfortunately, the crack branching angle and crack tip velocity at branching are

consistently lower than the above value (for a survey of the brittle fracture velocities, see Table 1 in [25]). It may be concluded, therefore, that the tendency of the maximum tangential stress $\sigma_{\theta\theta}$ to move out of the plane of crack propagation at higher velocities is at best a contributory factor to the branching event. In addition, it may be worthwhile to note that dynamic stress intensity factors (K_{ID}) are independent of the crack speed and the energy release rates go to infinity as the crack speed approaches the Rayleigh wave speed. This physical inconsistency was discussed by Rice [26]. Steady-state problems were also studied by Jahanshahi [27], Chen and Sih [28], and Sih and Loeber [29].

Broberg [30] and Baker [31] studied, first of all, the transient dynamic problems. Broberg [30] investigated a problem in which a crack initiates at a point and propagates symmetrically with constant velocity under constant pressure on the crack surface. It was found that the velocity of such a crack is equal to the Rayleigh wave velocity under the assumption of zero surface energy. Baker [31] investigated a semi-infinite crack which suddenly appears in a uniformly stretched elastic medium and then propagates with constant velocity by employing the Wiener-Hopf technique. The dynamic stress intensity factor K_{ID} is evaluated from the Baker's solution, presented in Appendix B for

comparison with the results of this investigation. Broberg's problem was reconsidered by Craggs [32], based on the self-similarity of the solutions. Attempts to remove the restriction of constant velocity of propagation were made by Kostrov [33] and Eshelby [34]. Kostrov [33] investigated unsteady propagation of a crack subjected to arbitrary time-dependent longitudinal shear loads on the crack surface using the method of Volterra. Eshelby [34] studied an analogous problem for quasi-static loads on the crack surface using Bateman's result on the electromagnetic radiation from a nonuniformly moving line charges. Eshelby's solution, however, can be obtained from Kostrov's solution, as mentioned in [19]. In [34], it was pointed out that if a propagating crack stops, a static field radiates out from the crack tip.

Achenbach [35] studied transient diffraction of horizontally polarized shear waves by a stationary semi-infinite crack by using the method of analysis in [33]. By introducing a fracture criterion based on the balance of energy, Achenbach showed that instantaneous crack propagation can occur only if the shear stress shows a square root singularity at the wave front. Achenbach and Nuismer [36] investigated diffraction of a time-dependent but spatially uniform dilatational wave by a semi-infinite crack propagating at constant speed and found similar results as in [35]. Freund

[37] considered a semi-infinite crack moving at constant speed under a unit concentrated load on the crack surface. Using this solution as a Green's function and adopting an inverse method, Freund derived K_{ID} for general static loads on the crack surface. He extended his work [38] to the case of nonuniform propagation of the crack and showed that K_{ID} is given by a function of instantaneous velocity times the corresponding static stress intensity factor (K_{IS}). For a suddenly stopping crack he found a result similar to Eshelby's [34]. Freund [39] also studied the case of stress wave loading and summarized his work in a review article [19]. In this article a suddenly stopping Broberg crack [30] was also considered.

Kostrov [40] extended his previous work [33] to any mode of loading conditions by means of the Wiener-Hopf technique. He verified Freund's [39] equation for K_{ID}. The case of a finite crack was also treated in [40], but no specific problem was considered. Glennie and Willis [41] studied an accelerating semi-infinite crack under a longitudinal shear load and presented an explicit expression for the elastodynamic field. They also discussed Griffith-Irwin fracture criterion and Dugdale-Barenblatt model in connection with acceleration of the crack.

The transient diffraction of dilatational waves by a stationary finite crack was investigated by Thau and

Lu [42]. They showed that the maximum value of K_{ID} is about 30 percent greater than the analogous K_{IS}, and the maximum value is attained at the instant of arrival of the first scattered Rayleigh wave from the opposite tip. The same problem was also considered by Sih, Embly and Ravera [43] in which they found that as time progresses, K_{ID} approaches K_{IS}, oscillating about it with decreasing amplitude, by using the Fredholm integral equation. Self-similar elastodynamic solutions associated with crack problems were reviewed by Cherepanov and Afanas'ev [44] with some applications, including Broberg's problem [30] and Baker's problem [31]. Kim [45] investigated the dynamic propagation of a finite crack in general terms for a stationary crack, a crack propagating at constant speed, and a crack which suddenly stops after propagation at constant speed. The method of solution is applicable to nonuniform rates of propagation of a crack under an arbitrary time-dependent load on the crack surface.

The fracture criterion for moving cracks similar to Griffith criterion under static equilibrium has been discussed by Erdogan [16], Atkinson and Eshelby [46], Achenbach [17] and Freund [19]. It has been shown in their work that the motion of a crack tip is determined by solving a complicated nonlinear ordinary differential equation for a given crack and loading condition. Ma and Burgers [47] studied the dynamic stress inten-

sity factor of an initially stationary semi-infinite crack in an unbounded linear elastic solid by using a perturbation method. The results indicated that if a maximum energy release rate is accepted as a crack propagation criterion, then for both the incident stress wave parallel to the original crack faces and uniform dynamic loading applied to the original crack faces, the crack will propagate straight ahead of the original crack for any delay time. Chattopadhyay and Bandyopadhyay [48] investigated the propagation of a crack due to shear waves in a medium having monoclinic symmetry. By using the Wiener-Hopf technique, it was shown that the stress intensity factor decreases as the length of the crack increases.

Numerical methods in dynamic fracture mechanics were critically appraised by Kanninen [49]. At that time, a comparison of the finite element and finite difference methods led to the following conclusions: The finite element method was more suitable for the analysis of stationary cracks under dynamic loadings due to the fact that the relevant singularities can be modeled in the crack tip elements. On the other hand, the finite element method was thought to be unsuited for the analysis of dynamic crack propagation, due to the numerical difficulties involved in advancing the crack in a discrete manner. However, the state of the technique of finite element methods in dynamic fracture

mechanics has greatly advanced in the intervening years. In order to simulate the crack propagation, two different concepts of computational modeling may be considered, namely, stationary mesh procedures [50,51, 52] and moving (distorting) mesh procedures [53,54,55]. The details were discussed in a review article by Atlury and Nishioka [56]. Also, Kishimoto, Aoki and Sakata [57,58] have derived a path-independent integral J for spatially fixed paths, which is equivalent to the energy release rate only for a stationary crack in a solid under dynamic loading. Recently, Banks-Sills [59] studied the quarter-point singular elements again and found that the quarter-point singular element should be rectangular rather than quadrilateral. Next, we briefly review some of the investigations concerning stress concentration around holes and also static fracture problems in micropolar elasticity.

Stress concentration around a circular hole in a plate was investigated by Kaloni and Ariman [60], who adopted the solution of the same problem for the indeterminate couple stress theory [61]. They showed that the solution given by Mindlin [61] can be obtained from the solution the obtained. Cowin [62] corrected the thermodynamic restrictions of Eringen's theory [13] and showed the results of the same problem for various values of coupling factors. The classical solutions of

the same problem coincides with the solutions [60,61, 62] when the coupling factor is zero.

The effect of couple stresses on the stress concentration at the crack tip of a crack was first considered by Muki and Sternberg [63], who treated the problem of a finite length crack in an infinite medium under conditions of plane strain with a uniform tension acting at infinity. Atkinson and Leppington [64] investigated the effect of couple stresses on the tip of a crack for a semi-infinite crack by using the Wiener-Hopf technique. Sladek and Sladek [65] and Paul and Sridharan [66] studied the effect of couple stresses on the stress field around a penny-shaped crack by solving a Fredholm integral equation of the second kind. An axisymmetric Boussinesq problem for a semi-space in micropolar media by means of Hankel transforms was studied by Dhaliwal and Khan [67]. Paul and Sridharan [68] investigated the problem of a Griffith crack in a transverse field of constant uniaxial tension by solving Fredholm integral equations of the second kind. From the above work, it was found that the stress intensity factor of the micropolar media is a little higher than that of classical media, and the energy release rate of the micropolar media is a little lower than that of classical media, as the coupling factor becomes higher.

Carbonaro and Russo [69] derived some classical theorems of micropolar elastodynamics in unbounded domains, namely, the work and energy theorem, the uniqueness and stability of regular solutions and a sufficient condition for the finiteness of the speed of propagation of signals (domain of influence theorem). Dai [70] extended the J-integral introduced by Rice [71] for micropolar media and Jaric and Suhubi [72] derived the Griffith criterion for brittle fracture within nonlinear micropolar thermoelasticity. Rao [73] investigated the problem of longitudinal wave propagation in a micropolar wave guide. It was seen that a new wave exists and the pattern of changes of this velocity is similar to those of SH-type of wave propagating in a wave guide. In addition, the micropolar counterpart of the Rayleigh-Lamb frequency equation was obtained, which can be reduced to the Rayleigh-Lamb equation of classical elasticity by neglecting the terms involving micropolar moduli.

Very little experimental work on micropolar materials has been done until now due to the lack of methods of measurement. Some work has been completed by Gauthier and Jahsman [74] for determination of micropolar moduli and by Yang and Lakes [75] on the stress intensity factor of bone. Numerical methods, such as finite element methods, have been developed by Malcolm

[76] for isotropic materials as well as orthotropic materials for the problem of determining the stress concentration around a hole. In static fracture mechanics of the micropolar theory of elasticity, many papers have been published, employing numerical techniques due to the complexity of the analysis involved. However, to the best of our knowledge, the problems of dynamic propagation of a finite crack in micropolar elastic media have not been investigated so far, either analytically or numerically.

CHAPTER 2

BASIC EQUATIONS IN MICROPOLAR ELASTICITY

In this chapter, the fundamental equations of micropolar elasticity are presented in a general curvilinear coordinate system and then are specialized to a rectangular coordinate system. The notations used are identical to those used by Eringen [77].

2.1 Field Equations

The field equations are obtained by combining the constitutive equations with the balance laws. There are two field equations, resulting in six partial differential equations for six unknowns (three displacements and three orientations) for problems with three-dimensional geometry. The field equations for micropolar, isotropic, homogeneous, linear elastic solids in an isothermal environment are

$$(\lambda+\mu)\nabla(\nabla\cdot\mathbf{u}) + (\mu+\kappa)\nabla^2\mathbf{u} + \kappa\,\nabla\times\boldsymbol{\phi} + \rho\mathbf{f} = \rho\ddot{\mathbf{u}} \tag{2.1.1}$$

and

$$(\alpha+\beta)\nabla(\nabla\cdot\boldsymbol{\phi}) + \gamma\nabla^2\boldsymbol{\phi} + \kappa\,\nabla\times\boldsymbol{\phi} - 2\kappa\boldsymbol{\phi} + \rho\boldsymbol{\ell} = \rho\mathbf{j}\ddot{\boldsymbol{\phi}}\,, \tag{2.1.2}$$

where $\mathbf{u}$ is the displacement field, $\boldsymbol{\phi}$ is the orientation field, and the superposed two dots on a vector denotes D^2/Dt^2. The quantities λ, μ, κ, α, β, and γ are the micropolar moduli; ρ and j are, respectively, the mass density and the microinertia density of the medium, which are treated as constants; and $\mathbf{f}$ and $\boldsymbol{\ell}$, respectively, are body force and the body couple per unit mass.

In a rectangular coordinate system, the field equations (2.1.1) and (2.1.2) become:

$$(\lambda+\mu)\frac{\partial}{\partial x}\left(\frac{\partial u_x}{\partial x}+\frac{\partial u_y}{\partial y}+\frac{\partial u_z}{\partial z}\right)+(\mu+\kappa)\left(\frac{\partial^2 u_x}{\partial x^2}+\frac{\partial^2 u_x}{\partial y^2}+\frac{\partial^2 u_x}{\partial z^2}\right)+\kappa\left(\frac{\partial \phi_z}{\partial y}-\frac{\partial \phi_y}{\partial z}\right)+\rho f_x=\rho\frac{\partial^2 u_x}{\partial t^2}, \qquad (2.1.3)$$

$$(\lambda+\mu)\frac{\partial}{\partial y}\left(\frac{\partial u_x}{\partial x}+\frac{\partial u_y}{\partial y}+\frac{\partial u_z}{\partial z}\right)+(\mu+\kappa)\left(\frac{\partial^2 u_y}{\partial x^2}+\frac{\partial^2 u_y}{\partial y^2}+\frac{\partial^2 u_y}{\partial z^2}\right)+\kappa\left(\frac{\partial \phi_x}{\partial z}-\frac{\partial \phi_z}{\partial x}\right)+\rho f_y=\rho\frac{\partial^2 u_y}{\partial t^2}, \qquad (2.1.4)$$

$$(\lambda+\mu)\frac{\partial}{\partial z}\left(\frac{\partial u_x}{\partial x}+\frac{\partial u_y}{\partial y}+\frac{\partial u_z}{\partial z}\right)+(\mu+\kappa)\left(\frac{\partial^2 u_z}{\partial x^2}+\frac{\partial^2 u_z}{\partial y^2}+\frac{\partial^2 u_z}{\partial z^2}\right)+\kappa\left(\frac{\partial \phi_y}{\partial x}-\frac{\partial \phi_x}{\partial y}\right)+\rho f_z=\rho\frac{\partial^2 u_z}{\partial t^2}, \qquad (2.1.5)$$

$$(\alpha+\beta)\frac{\partial}{\partial x}\left(\frac{\partial \phi_x}{\partial x}+\frac{\partial \phi_y}{\partial y}+\frac{\partial \phi_z}{\partial z}\right)+(\mu+\kappa)\left(\frac{\partial^2 \phi_x}{\partial x^2}+\frac{\partial^2 \phi_x}{\partial y^2}+\frac{\partial^2 \phi_x}{\partial z^2}\right)+\kappa\left(\frac{\partial \phi_z}{\partial y}-\frac{\partial \phi_y}{\partial z}\right)-2\kappa\phi_z$$

$$+\rho\ell_x=\rho j\frac{\partial^2 \phi_x}{\partial t^2}, \qquad (2.1.6)$$

$$(\alpha+\beta)\frac{\partial}{\partial y}\left(\frac{\partial \phi_x}{\partial x}+\frac{\partial \phi_y}{\partial y}+\frac{\partial \phi_z}{\partial z}\right)+(\mu+\kappa)\left(\frac{\partial^2 \phi_y}{\partial x^2}+\frac{\partial^2 \phi_y}{\partial y^2}\right.$$

$$\left.\frac{\partial^2 \phi_y}{\partial z^2}\right)+\kappa\left(\frac{\partial \phi_x}{\partial z}-\frac{\partial \phi_z}{\partial x}\right)-2\kappa\phi_y$$

$$+\rho \ell_y=\rho j \frac{\partial^2 \phi_y}{\partial t^2} . \qquad (2.1.7)$$

and

$$(\alpha+\beta)\frac{\partial}{\partial z}\left(\frac{\partial \phi_x}{\partial x}+\frac{\partial \phi_y}{\partial y}+\frac{\partial \phi_z}{\partial z}\right)+(\mu+\kappa)\left(\frac{\partial^2 \phi_z}{\partial x^2}+\frac{\partial^2 \phi_z}{\partial y^2}\right.$$

$$\left.\frac{\partial^2 \phi_z}{\partial z^2}\right)+\kappa\left(\frac{\partial \phi_y}{\partial z}-\frac{\partial \phi_x}{\partial x}\right)-2\kappa\phi_x$$

$$+\rho \ell_z=\rho j \frac{\partial^2 \phi_z}{\partial t^2} . \qquad (2.1.8)$$

2.2 Equilibrium Equations

The equilibrium equations used in micropolar elasticity are the equation of momentum and the equation of moment of momentum. The equation of momentum is identical to that of classical elasticity and is written as

$$\nabla \cdot \mathbf{t} + \rho(\mathbf{f}-\dot{\mathbf{v}}) = \mathbf{0} , \qquad (2.2.1)$$

where $\mathbf{v}$ is the velocity vector, $\mathbf{t}$ is the stress tensor and a dot superposed on a vector denotes its material time rate. The equation of moment of momentum in micropolar elasticity is different from that of classical elasticity and is written as

$$\nabla \cdot \mathbf{m} + (\mathbf{t}-\mathbf{t}^T) + \rho(\ell-\dot{\sigma}) = \mathbf{0} , \qquad (2.2.2)$$

where $\mathbf{m}$ is the couple stress tensor, $\boldsymbol{\sigma}$ is the spin tensor and the superposed T over a tensor denotes its transpose.

Equations (2.2.1) and (2.2.2) can be written in a rectangular coordinate system as

$$\frac{\partial t_{xx}}{\partial x} + \frac{\partial t_{yx}}{\partial y} + \frac{\partial t_{zx}}{\partial z} + \rho(f_x - \dot{v}_x) = 0 \quad , \tag{2.2.3}$$

$$\frac{\partial t_{xy}}{\partial x} + \frac{\partial t_{yy}}{\partial y} + \frac{\partial t_{zy}}{\partial z} + \rho(f_y - \dot{v}_y) = 0 \quad , \tag{2.2.4}$$

$$\frac{\partial t_{xz}}{\partial x} + \frac{\partial t_{yz}}{\partial y} + \frac{\partial t_{zz}}{\partial z} + \rho(f_z - \dot{v}_z) = 0 \quad , \tag{2.2.5}$$

and

$$\frac{\partial m_{xx}}{\partial x} + \frac{\partial m_{yx}}{\partial y} + \frac{\partial m_{zx}}{\partial z} + t_{yz} - t_{zy} + \rho(\ell_x - \dot{\sigma}_x) = 0 \quad , \tag{2.2.6}$$

$$\frac{\partial m_{xy}}{\partial x} + \frac{\partial m_{yy}}{\partial y} + \frac{\partial m_{zy}}{\partial z} + t_{zx} - t_{xz} + \rho(\ell_y - \dot{\sigma}_y) = 0 \quad , \tag{2.2.7}$$

and

$$\frac{\partial m_{xz}}{\partial x} + \frac{\partial m_{yz}}{\partial y} + \frac{\partial m_{zz}}{\partial z} + t_{xy} - t_{yx} + \rho(\ell_z - \dot{\sigma}_z) = 0 \quad . \tag{2.2.8}$$

2.3 Constitutive Equations

The constitutive equations for micropolar elasticity consist of a stress constitutive equation involving microrotation, and a couple stress constitutive equation involving the gradients of microrotation.

2.3.1 The Stress Constitutive Equation

The stress constitutive equation may be written in two alternate forms:

$$t_{k\ell} = \lambda \epsilon^{m}{}_{m} g_{k\ell} + (\mu+\kappa)\epsilon_{k\ell} + \mu \epsilon_{\ell k} \qquad (2.3.1)$$

or

$$t_{k\ell} = \lambda e^{m}{}_{m} g_{k\ell} + (2\mu+\kappa)e_{k\ell} + \kappa e_{k\ell m}(r^{m}-\phi^{m}) \quad , (2.3.2)$$

where

$$\phi^{k} = -(1/2)e^{k\ell m}\phi_{\ell m} \quad ,$$

$$e_{k\ell} = (1/2)(u_{k;\ell} + u_{\ell;k}) \quad ,$$

$$\epsilon_{k\ell} = \phi_{k\ell} + u_{\ell;k} = e_{k\ell} + e_{k\ell m}(r^{m}-\phi^{m}) \quad ,$$

$$r^{k} = (1/2)e^{k\ell m}r_{m\ell} = (1/2)e^{k\ell m}u_{m,\ell} \quad ,$$

and where $\epsilon^{m}{}_{m}$ is obtained by raising the index in $\epsilon_{k\ell}$ with the fundamental matrix tensor and then contracting it; $g_{k\ell}$ is the coefficient of the fundamental matrix, r^{k} is the classical rotation vector, $e_{k\ell}$ and $\epsilon_{k\ell}$ are, respectively, the classical strain tensor and Cosserat strain tensor, $e_{k\ell m}$ is the alternating tensor and ";" denotes the covariant partial derivative.

Equations (2.3.1) or (2.3.2) lead to nine stress constitutive equations using equations in rectangular coordinate systems:

$$t_{xx} = (\lambda+2\mu+\kappa)\frac{\partial u_x}{\partial x} + \lambda\left(\frac{\partial u_y}{\partial y} + \frac{\partial u_z}{\partial z}\right) \quad , \qquad (2.3.3)$$

$$t_{xy} = (\mu+\kappa)\frac{\partial u_y}{\partial x} + \mu\frac{\partial u_x}{\partial y} - \kappa\phi_z \quad , \qquad (2.3.4)$$

$$t_{xz} = (\mu+\kappa)\frac{\partial u_z}{\partial x} + \mu\frac{\partial u_x}{\partial z} + \kappa\phi_y \ , \qquad (2.3.5)$$

$$t_{yx} = (\mu+\kappa)\frac{\partial u_x}{\partial y} + \mu\frac{\partial u_y}{\partial x} + \kappa\phi_z \ , \qquad (2.3.6)$$

$$t_{yy} = (\lambda+2\mu+\kappa)\frac{\partial u_y}{\partial y} + \lambda\left(\frac{\partial u_x}{\partial x} + \frac{\partial u_z}{\partial z}\right) \ , \qquad (2.3.7)$$

$$t_{yz} = (\mu+\kappa)\frac{\partial u_z}{\partial y} + \mu\frac{\partial u_y}{\partial z} - \kappa\phi_x \ , \qquad (2.3.8)$$

$$t_{zx} = (\mu+\kappa)\frac{\partial u_x}{\partial z} + \mu\frac{\partial u_z}{\partial x} - \kappa\phi_y \ , \qquad (2.3.9)$$

$$t_{zy} = (\mu+\kappa)\frac{\partial u_y}{\partial z} + \mu\frac{\partial u_z}{\partial y} + \kappa\phi_x \qquad (2.3.10)$$

and

$$t_{zz} = (\lambda+2\mu+\kappa)\frac{\partial u_z}{\partial z} + \lambda\left(\frac{\partial u_x}{\partial x} + \frac{\partial u_y}{\partial y}\right) \ . \qquad (2.3.11)$$

2.3.2 The Couple Stress Constitutive Equation

The couple stress constitutive equation is written as

$$m_{k\ell} = \alpha\phi^r{}_{;r}g_{k\ell} + \beta\phi_{k;\ell} + \gamma\phi_{\ell;k} \ . \qquad (2.3.12)$$

In a rectangular coordinate system, the nine couple stress constitutive equations are:

$$m_{xx} = (\alpha+\beta+\gamma)\frac{\partial \phi_x}{\partial x} + \alpha\left(\frac{\partial \phi_y}{\partial y} + \frac{\partial \phi_z}{\partial z}\right) \ , \qquad (2.3.13)$$

$$m_{xy} = \beta\frac{\partial \phi_x}{\partial y} + \gamma\frac{\partial \phi_y}{\partial x} \ , \qquad (2.3.14)$$

$$m_{xz} = \beta\frac{\partial \phi_x}{\partial z} + \gamma\frac{\partial \phi_z}{\partial x} \ , \qquad (2.3.15)$$

$$m_{yx} = \beta\frac{\partial\phi_y}{\partial x} + \gamma\frac{\partial\phi_x}{\partial y} , \tag{2.3.16}$$

$$m_{yy} = (\alpha+\beta+\gamma)\frac{\partial\phi_y}{\partial y} + \alpha\left(\frac{\partial\phi_x}{\partial x} + \frac{\partial\phi_z}{\partial z}\right) , \tag{2.3.17}$$

$$m_{yz} = \beta\frac{\partial\phi_y}{\partial z} + \gamma\frac{\partial\phi_z}{\partial y} , \tag{2.3.18}$$

$$m_{zx} = \beta\frac{\partial\phi_z}{\partial x} + \gamma\frac{\partial\phi_x}{\partial z} , \tag{2.3.19}$$

$$m_{zy} = \beta\frac{\partial\phi_z}{\partial y} + \gamma\frac{\partial\phi_y}{\partial z} \tag{2.3.20}$$

and

$$m_{zz} = (\alpha+\beta+\gamma)\frac{\partial\phi_z}{\partial z} + \alpha\left(\frac{\partial\phi_x}{\partial x} + \frac{\partial\phi_y}{\partial y}\right) . \tag{2.3.21}$$

2.4 Compatibility Equations

The compatibility equations are used to insure the compatibility of displacements and orientations of specific solutions in micropolar elasticity. The micropolar strain tensors involve gradients of displacements and micro-orientations and the compatibility equations insure their existence as well as consistency. In general, a set of displacements and micro-orientations will not exist unless the strains satisfy certain conditions. Mathematically, the compatibility equations are necessary and sufficient conditions for the continuity and single-valuedness of displacements and micro-orientations.

The compatibility equation is given by

$$\epsilon_{ik;j} - \epsilon_{jk;i} + \gamma_{ikj} - \gamma_{jki} = 0 \ , \qquad (2.4.1)$$

where

$$\gamma_{k\ell m} = e_{k\ell n}\phi^{n};_{m} \ . \qquad (2.4.2)$$

Using the definition of $\gamma_{k\ell m}$, one can express equation (2.4.2) in the form

$$\epsilon_{ik;j} - \epsilon_{jk;i} + e_{ikn}\phi^{n};_{j} - e_{jkm}\phi^{m};_{i} = 0 \ . \qquad (2.4.3)$$

In a rectangular coordinate system, equation (2.4.3) results in 27 equations, of which 9 prove trivial and 9 out of the remaining 18 equations are repetitious. The remaining independent three-dimensional compatibility equations in the rectangular coordinate system are:

$$\frac{\partial \epsilon_{xx}}{\partial y} - \frac{\partial \epsilon_{yx}}{\partial x} + \frac{\partial \phi_z}{\partial x} = 0 \ , \qquad (2.4.4)$$

$$\frac{\partial \epsilon_{xy}}{\partial y} - \frac{\partial \epsilon_{yy}}{\partial x} + \frac{\partial \phi_z}{\partial y} = 0 \ , \qquad (2.4.5)$$

$$\frac{\partial \epsilon_{xz}}{\partial y} - \frac{\partial \epsilon_{yz}}{\partial x} - \frac{\partial \phi_y}{\partial y} - \frac{\partial \phi_x}{\partial x} = 0 \ , \qquad (2.4.6)$$

$$\frac{\partial \epsilon_{xx}}{\partial z} - \frac{\partial \epsilon_{zx}}{\partial x} - \frac{\partial \phi_y}{\partial x} = 0 \ , \qquad (2.4.7)$$

$$\frac{\partial \epsilon_{xy}}{\partial z} - \frac{\partial \epsilon_{zy}}{\partial x} + \frac{\partial \phi_z}{\partial z} + \frac{\partial \phi_x}{\partial x} = 0 \ , \qquad (2.4.8)$$

$$\frac{\partial \epsilon_{xz}}{\partial z} - \frac{\partial \epsilon_{zz}}{\partial x} - \frac{\partial \phi_y}{\partial z} = 0 \ , \qquad (2.4.9)$$

$$\frac{\partial \epsilon_{yx}}{\partial z} - \frac{\partial \epsilon_{zx}}{\partial y} - \frac{\partial \phi_z}{\partial z} - \frac{\partial \phi_y}{\partial y} = 0 \ , \qquad (2.4.10)$$

$$\frac{\partial \epsilon_{yy}}{\partial z} - \frac{\partial \epsilon_{zy}}{\partial y} + \frac{\partial \phi_x}{\partial y} = 0 \ , \tag{2.4.11}$$

and

$$\frac{\partial \epsilon_{yz}}{\partial z} - \frac{\partial \epsilon_{zz}}{\partial y} + \frac{\partial \phi_x}{\partial z} = 0 \ . \tag{2.4.12}$$

where

$$\epsilon_{xx} = \frac{\partial u_x}{\partial x} \ , \quad \epsilon_{yy} = \frac{\partial u_y}{\partial y} \ , \quad \epsilon_{zz} = \frac{\partial u_z}{\partial z} \ ,$$

$$\epsilon_{xy} = \frac{\partial u_y}{\partial x} - \phi_z \ , \quad \epsilon_{yx} = \frac{\partial u_x}{\partial y} + \phi_z \ ,$$

$$\epsilon_{yz} = \frac{\partial u_z}{\partial y} - \phi_x \ , \quad \epsilon_{zy} = \frac{\partial u_y}{\partial z} + \phi_x \ ,$$

$$\epsilon_{zx} = \frac{\partial u_x}{\partial z} - \phi_y \ , \quad \epsilon_{xz} = \frac{\partial u_z}{\partial x} + \phi_y \ . \tag{2.4.13}$$

Additional compatibility equations result from examining the couple stress constitutive equations as they arise in plane problems. Since $\boldsymbol{\phi} = (0,0,\phi_z)$ for the x-y plane, equations (2.3.15) and (2.3.18) become

$$m_{xz} = \gamma \frac{\partial \phi_z}{\partial x} \ , \tag{2.4.14}$$

and

$$m_{yz} = \gamma \frac{\partial \phi_z}{\partial y} \ , \tag{2.4.15}$$

Cross differentiation of equations (2.4.14) and (2.4.15), followed by subtraction of (2.4.15) from (2.4.14), results in

$$\frac{\partial m_{xz}}{\partial y} - \frac{\partial m_{yz}}{\partial x} = 0 \ . \tag{2.4.16}$$

Likewise, for the y-z plane, we get

$$\frac{\partial m_{yx}}{\partial z} - \frac{\partial m_{zx}}{\partial y} = 0 \qquad (2.4.17)$$

and for the x-z plane, we get

$$\frac{\partial m_{xy}}{\partial z} - \frac{\partial m_{zy}}{\partial x} = 0 \ . \qquad (2.4.18)$$

Another compatibility condition which assures the single valuedness as well as continuity of microrotation is expressed in the rectangular coordinate system as

$$e_{k\ell z}(\gamma_{k\ell m,n} - \gamma_{k\ell n,m}) = 0 \ , \qquad (2.4.19)$$

where

$$\gamma_{k\ell m,n} = e_{k\ell p}\phi_{p,mn} \ . \qquad (2.4.20)$$

CHAPTER 3

DESCRIPTION AND ANALYSIS OF THE PROBLEM

3.1 Statement of Problem

A plane finite crack is contained in an unbounded medium as shown in Figure 1. The body is micropolar, linearly elastic, isotropic and homogeneous, and the body force and the body couple are assumed to be negligible. A Cartesian coordinate system which has been normalized by the half crack length is introduced in such a way that the crack surface is initially defined by $-1 < x < 1$, $y = 0\pm$, $-\infty < z < \infty$. The time variable used in this study has also been normalized by the time for the micropolar dilatational wave to travel half of the crack length. As a result of this normalization, the micropolar dilatational wave speed is equal to unity. The propagation distances of the right and left crack tips are denoted by $a_+(t)$ and $a_-(t)$, respectively. Thus, the positions of the crack tips at time, t, are given by $x = \pm 1 \pm a_\pm(t)$, $y = 0\pm$.

The crack tip velocities $c_\pm(t)$ are such that $c_\pm(t) = 0$ for $t < 0$ and $0 < c_\pm(t) < C_R$ for $t \geq 0$, where

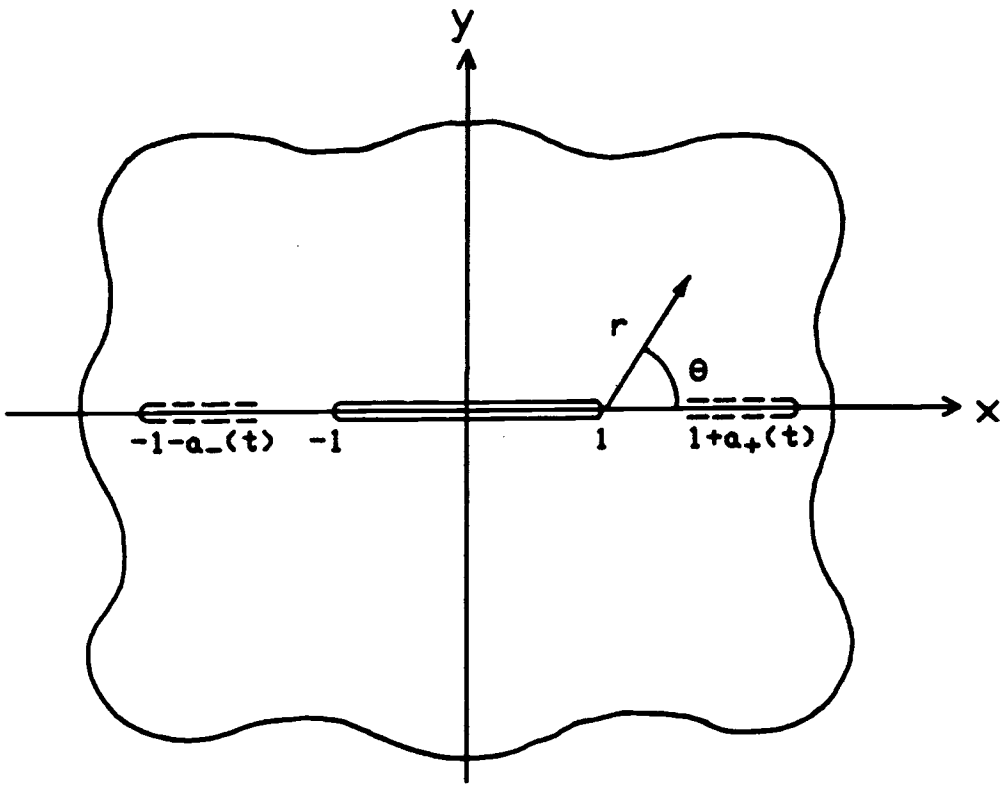

Figure 1. Geometry of the Problem.

C_R is the micropolar Rayleigh wave speed. The field equations of micropolar linear elasticity are

$$(C_D^2+C_3^2)u_{,xx} + (C_D^2-C_S^2)v_{,xy} + (C_S^2+C_3^2)u_{,yy} + C_3^2\phi_{,y} = u_{,tt} , \qquad (3.1.1)$$

$$(C_D^2+C_3^2)v_{,xx} + (C_D^2-C_S^2)u_{,xy} + (C_S^2+C_3^2)v_{,yy} + C_3^2\phi_{,x} = v_{,tt} , \qquad (3.1.2)$$

and

$$C_4^2(\phi_{,xx}+\phi_{,yy}) + \frac{C_3^2}{j}(v_{,x}-u_{,y}) - \frac{2}{j}C_3^2\phi = \phi_{,tt} , \qquad (3.1.3)$$

where u and v are the x- and y- components of the displacement vector and ϕ is the z-component of the microrotation vector, and

$$C_D^2 = \frac{\lambda+2\mu}{\rho} , \quad C_S^2 = \frac{\mu}{\rho} , \quad C_3^2 = \frac{\kappa}{\rho} , \quad C_4^2 = \frac{\gamma}{\rho j} .$$

The quantities λ, μ, κ and γ are the micropolar moduli, and ρ and j are the mass density and the microinertia density, respectively, of the medium, and are treated as constants.

The general solution of this problem is the superposition of the solutions to the following: (1) the problem of the crack-free region subjected to uniaxial tension, $\sigma(x,t)$, and (2) the problem of the crack opened out by normal pressure, $\sigma(x,t)$, with no loading at infinity. Since we are interested in the dynamic stress and couple stress intensity factors, only problem (2) is considered since both of the stress inten-

sity factors may be derived from it. By symmetry, this problem is equivalent to the problem of determination of stress distribution in the half plane $y \geq 0$, when its boundary is subjected to the following conditions:

$$\left.\begin{aligned} t_{yy}(x,0,t) &= -\sigma(x,t) \\ M_{yz}(x,0,t) &= 0 \end{aligned}\right\} \quad -1-a_-(t) < x < 1+a_+(t) , \qquad (3.1.4)\ (3.1.5)$$

$$\left.\begin{aligned} v(x,0,t) &= 0 \\ \phi(x,0,t) &= 0 \end{aligned}\right\} \quad x > 1 + a_+(t) \text{ or } x < -1-a_-(t) , \qquad (3.1.6)\ (3.1.7)$$

and

$$t_{yx}(x,0,t) = 0 \qquad 0 \leq |x| < \infty , \qquad (3.1.8)$$

where t_{yy}, t_{yx}, σ and M_{yz} represent, respectively, the normal stress component, the shear stress component, the uniaxial tension, and pertinent couple stress component, normalized with respect to the shear modulus of the material. The initial conditions are

$$\begin{aligned} u(x,y,0) &= 0 , \\ v(x,y,0) &= 0 , \\ \phi(x,y,0) &= 0 , \\ u_{,t}(x,y,0) &= 0 , \\ v_{,t}(x,y,0) &= 0 , \\ \phi_{,t}(x,y,0) &= 0 \end{aligned} \qquad (3.1.9)$$

for all x and y.

The components of stress, displacement and microrotation must vanish as $(x^2+y^2) \to \infty$. Moreover, the symmetry with respect to the y-axis provides the additional conditions,

$$v(x,0,t) = v(-x,0,t) \ ,$$
$$\phi(x,0,t) = -\phi(-x,0,t) \ . \qquad -\infty < x < \infty \ , \quad (3.1.10)$$

3.2 Solution in Transform Space

Since the problem is symmetric with respect to $y = 0$, only the upper half space is considered and $y = 0$ is used rather than $y = 0+$ for the y-coordinate of the crack surface. Integral transforms are employed to reduce the partial differential equations (3.1.1)-(3.1.3) to ordinary differential equations. First, the time, t, is eliminated by application of the Laplace transform,

$$\bar{f}(x,y,p) = \int_0^\infty f(x,y,t)e^{-pt}dt \ , \qquad (3.2.1)$$

where p is a positive real number. It is assumed that equation (3.2.1) exists for any point (x,y) in the material. The initial conditions (3.1.9) are used in this transform. Second, Fourier trigonometric transforms are used to suppress y. They are defined by

$$\hat{\bar{f}}(x,s,p) = \int_0^\infty \bar{f}(x,y,p) \cos(sy)\, dy$$

and

$$\tilde{\bar{f}}(x,s,p) = \int_0^\infty \bar{f}(x,y,p) \sin(sy)\, dy \ . \qquad (3.2.2)$$

The Fourier cosine transform is applied to the Laplace transform of equation (3.1.1) and a Fourier sine trans-

form is applied, respectively, to the Laplace transform of equations (3.1.2) and (3.1.3). The resulting equations are

$$\hat{\bar{u}}_{,xx} - (A^2s^2+p^2)\hat{\bar{u}} + B^2s\tilde{\bar{v}}_{,x} + sC^2\tilde{\bar{\phi}} = (B^2+C^2-A^2)\bar{v}_{,x} , \tag{3.2.3}$$

$$A^2\tilde{\bar{v}}_{,xx} - (s^2+p^2)\tilde{\bar{v}} - B^2s\hat{\bar{u}}_{,x} - C^2\tilde{\bar{\phi}}_{,x} = -s\bar{v} , \tag{3.2.4}$$

and

$$\theta^2\tilde{\bar{\phi}}_{,xx} - (\theta^2s^2+\frac{2\epsilon}{j}+\frac{p^2}{C_2^2})\tilde{\bar{\phi}} + \frac{\epsilon}{j}(s\hat{\bar{u}}+\tilde{\bar{v}},x) = -\theta^2s\bar{\phi} , \tag{3.2.5}$$

where

$$A^2 = \frac{C_s^2+C_3^2}{C_M},\ B^2 = \frac{C_D^2-C_s^2}{C_M},\ C^2 = \frac{C_3^2}{C_M},\ \epsilon = \frac{C_3^2}{C_s^2} ,$$

$$\theta^2 = \frac{C_4^2}{C_s^2} = \frac{\gamma}{\mu j},\ C_2^2 = \frac{C_s^2}{C_M},\ C_M = C_D^2+C_3^2 . \tag{3.2.6}$$

Boundary condition (3.1.8) has been used to obtain the right-hand sides of equations (3.2.3) and (3.3.4) in terms of $\bar{v}(x,0,p)$ and $\bar{v}_{,x}(x,0,p)$.

The general solutions of equation (3.2.3)-(3.2.5) are given by

$$\begin{aligned}\hat{\bar{u}}(x,s,p) = {} & B_1(s,p)e^{\gamma_1 x} + B_2(s,p)e^{-\gamma_1 x} + B_3(s,p)e^{\gamma_2 x} \\ & + B_4(s,p)e^{-\gamma_2 x} + B_5(s,p)e^{\gamma_3 x} + B_6(s,p)e^{-\gamma_3 x} \\ & + T_3\int_{-\infty}^{x}\bar{v}(\eta,0,p)\cosh[\gamma_3(\eta-x)]\,d\eta \\ & + T_2\int_{-\infty}^{x}\bar{v}(\eta,0,p)\cosh[\gamma_2(\eta-x)]\,d\eta\end{aligned}$$

$$+ T_1 \int_{-\infty}^{x} \bar{v}(\eta,0,p) \cosh[\gamma_1(\eta-x)]\, d\eta$$

$$+ t_3 \int_{-\infty}^{x} \bar{\phi}(\eta,0,p) \sinh[\gamma_3(\eta-x)]\, d\eta$$

$$+ t_2 \int_{-\infty}^{x} \bar{\phi}(\eta,0,p) \sinh[\gamma_2(\eta-x)]\, d\eta \ , \qquad (3.2.7)$$

$$\tilde{v}(x,s,p) = -\frac{s}{\gamma_1} B_1(s,p) e^{\gamma_1 x} + \frac{s}{\gamma_1} B_2(s,p) e^{-\gamma_1 x}$$

$$- \frac{\gamma_2}{s} B_3(s,p) e^{\gamma_2 x} + \frac{\gamma_2}{s} B_4(s,p) e^{-\gamma_2 x}$$

$$- \frac{\gamma_3}{s} B_5(s,p) e^{\gamma_3 x} + \frac{\gamma_3}{s} B_6(s,p) e^{-\gamma_3 x}$$

$$+ V_3 \int_{-\infty}^{x} \bar{v}(\eta,0,p) \sinh[\gamma_3(\eta-x)]\, d\eta$$

$$+ V_2 \int_{-\infty}^{x} \bar{v}(\eta,0,p) \sinh[\gamma_2(\eta-x)]\, d\eta$$

$$+ V_1 \int_{-\infty}^{x} \bar{v}(\eta,0,p) \sinh[\gamma_1(\eta-x)]\, d\eta$$

$$+ V'_3 \int_{-\infty}^{x} \bar{\phi}(\eta,0,p) \cosh[\gamma_3(\eta-x)]\, d\eta$$

$$+ V'_2 \int_{-\infty}^{x} \bar{\phi}(\eta,0,p) \cosh[\gamma_2(\eta-x)]\, d\eta \ , \qquad (3.2.8)$$

and

$$\tilde{\phi}(x,s,p) = F_2 B_3(s,p) e^{\gamma_2 x} + F_2 B_4(s,p) e^{-\gamma_2 x}$$

$$+ F_3 B_5(s,p) e^{\gamma_3 x} + F_3 B_6(s,p) e^{-\gamma_3 x}$$

$$+ W_3 \int_{-\infty}^{x} \bar{v}(\eta,0,p) \cosh[\gamma_3(\eta-x)]\, d\eta$$

$$+ W_2 \int_{-\infty}^{x} \bar{v}(\eta,0,p) \cosh[\gamma_2(\eta-x)]\, d\eta$$

$$+ W_1 \int_{-\infty}^{x} \bar{v}(\eta,0,p) \cosh[\gamma_1(\eta-x)]\, d\eta$$

$$+ W'_3 \int_{-\infty}^{x} \bar{\phi}(\eta,0,p) \sinh[\gamma_3(\eta-x)]\, d\eta$$

$$+ W'_2 \int_{-\infty}^{x} \bar{\phi}(\eta,0,p) \sinh[\gamma_2(\eta-x)]\, d\eta \ , \qquad (3.2.9)$$

where

$$\gamma_1^2 = s^2 + p^2 \ ,$$

$$\gamma_2^2 = s^2 + \frac{p^2}{2\theta^2A^2}(A^2/C_2^2+\theta^2B^2-\theta^2A^2) + \frac{\epsilon}{j}\frac{(2A^2-C^2)}{2\theta^2A^2} - R^{1/2} \ ,$$

$$\gamma_3^2 = s^2 + \frac{p^2}{2\theta^2A^2}(A^2/C_2^2+\theta^2B^2-\theta^2A^2) + \frac{\epsilon}{j}\frac{(2A^2-C^2)}{2\theta^2A^2} + R^{1/2} \ ,$$

$$R = [p^2(A^2/C_2^2-\theta^2)+\epsilon/j(2A^2-C^2)]^2 - 4\epsilon\theta^2C^2p^2/j \ ,$$

$$T_1 = -\frac{1}{p^2}(-\gamma_1^2L^2+s^2) \ ,$$

$$T_2 = -\frac{1}{\theta^2A^2}\frac{1}{\gamma_3^2-\gamma_2^2}(R_5\gamma_2^2+R_5\gamma_1^2+R_3+\frac{T}{\gamma_2^2-\gamma_1^2}) \ ,$$

$$T_3 = L^2 - T_2 - T_1 \ ,$$

$$t_2 = \frac{\theta^2s^2C^2}{\gamma_2}\frac{1}{\gamma_3^2-\gamma_2^2}\frac{1}{\theta^2A^2} \ ,$$

$$t_3 = -\frac{\theta^2s^2C^2}{\gamma_3}\frac{1}{\gamma_3^2-\gamma_2^2}\frac{1}{\theta^2A^2} \ ,$$

$$V_1 = \frac{1}{s}\left[\gamma_1 T_1 - \gamma_1 L^2 + \frac{s^2}{\gamma_1}\right] ,$$

$$V_i = \gamma_i T_i / s \qquad (i = 2,3) ,$$

$$V'_i = \gamma_i t_i / s \qquad (i = 2,3) ,$$

$$W_i = -\{\gamma_i{}^2 T_i - (A^2 s^2 + p^2) T_i - \gamma_i B^2 s V_i\}/sC^2 \quad (i=1,2,3) ,$$

$$W'_i = -\{\gamma_i{}^2 t_i - (A^2 s^2 + p^2) t_i - \gamma_i B^2 s V'_i\}/sC^2 \quad (i=2,3) ,$$

$$R_5 = \theta^2 A^2 L^2 ,$$

$$L^2 = B^2 + C^2 - A^2 ,$$

$$R_3 = \theta^2 s^2 (B^2 - L^2 - A^2 L^2) - p^2 L^2 \left[\theta^2 + \frac{A^2}{C_2{}^2}\right] - \frac{\epsilon L^2}{j}(2A^2 - C^2) ,$$

$$R_1 = \theta^2 s^4 (L^2 - B^2) + s^2 p^2 \left[\theta^2 L^2 + \frac{L^2 - B^2}{C_2{}^2}\right] + \frac{L^2}{C_2{}^2} p^4 + \frac{\epsilon s^2}{j}(2L^2 - C^2) + \frac{2\epsilon}{j} L^2 p^2 ,$$

and

$$F_i = (-B^2 s^2 - A^2 \gamma_i{}^2 + \gamma_1{}^2)/sC^2 \qquad (i=2,3) . \quad (3.2.10)$$

The coefficients $B_i (i=1,2,..,6)$ are determined from the following conditions:

$$\left.\begin{aligned} \hat{\bar{u}}(x,s,p) &= 0 \\ \tilde{\bar{v}}(x,s,p) &= 0 \\ \tilde{\bar{\phi}}(x,s,p) &= 0 \end{aligned}\right\} \qquad \text{at } x = \pm\infty . \qquad (3.2.11)$$

We get

$$B_1(s,p) = -\frac{T_1}{2}\int_{-\infty}^{\infty} \bar{v}(\eta,0,p) e^{-\gamma_1 \eta} d\eta ,$$

$$B_3(s,p) = -\frac{T_2}{2}\int_{-\infty}^{\infty}\bar{v}(\eta,0,p)e^{-\gamma_2\eta}d\eta\ ,$$

$$+\frac{t_2}{2}\int_{-\infty}^{\infty}\bar{\phi}(\eta,0,p)e^{-\gamma_2\eta}d\eta\ ,$$

$$B_5(s,p) = -\frac{T_3}{2}\int_{-\infty}^{\infty}\bar{v}(\eta,0,p)e^{-\gamma_3\eta}d\eta\ ,$$

$$+\frac{t_3}{2}\int_{-\infty}^{\infty}\bar{\phi}(\eta,0,p)e^{-\gamma_3\eta}d\eta\ ,$$

$$B_2(s,p) = B_4(s,p) = B_6(s,p) = 0\ . \qquad (3.2.12)$$

The stress components in the transform space, $\hat{\bar{t}}_{xx}$, $\hat{\bar{t}}_{yy}$, $\tilde{\bar{t}}_{yx}$, $\tilde{\bar{M}}_{xz}$, and $\hat{\bar{M}}_{yz}$ can then be obtained by transforming the stress-displacement equations and substituting for $\hat{\bar{u}}$, $\tilde{\bar{v}}$, and $\tilde{\bar{\phi}}$ from equations (3.2.7)-(3.2.9). However, only $\hat{\bar{t}}_{yy}$ and $\hat{\bar{M}}_{yz}$ are considered since the main object of this study is the determination of the dynamic stress and couple stress intensity factors. The transformed, normalized stress component $\hat{\bar{t}}_{yy}$ is given by

$$\hat{\bar{t}}_{yy}(x,s,p) = \frac{1}{C_2{}^2}\left[-\bar{v}(x,0,p)+s\tilde{\bar{v}}(x,s,p)\right]$$

$$+\frac{L^2}{C_2{}^2}\hat{\bar{u}},_x\ . \qquad (3.2.13)$$

Substituting $\hat{\bar{u}}$ and $\tilde{\bar{v}}$ from equations (3.2.7) and (3.2.8) into the equation (3.2.13) and integrating by parts, we obtain

$$\hat{\bar{t}}_{yy}(x,s,p) =$$

$$-\frac{T_1}{2}(L^2-s^2/\gamma_1{}^2)\int_x^{\infty}\bar{v},_\eta(\eta,0,p)e^{-\gamma_1(\eta-x)}d\eta$$

$$+\frac{T_1}{2}(L^2-s^2/\gamma_1{}^2)\int_{-\infty}^{x}\bar{v}_{,\eta}(\eta,0,p)e^{\gamma_1(\eta-x)}d\eta$$

$$-\frac{T_2}{2}(L^2-1)\int_{x}^{\infty}\bar{v}_{,\eta}(\eta,0,p)e^{-\gamma_2(\eta-x)}d\eta$$

$$+\frac{T_2}{2}(L^2-1)\int_{-\infty}^{x}\bar{v}_{,\eta}(\eta,0,p)e^{\gamma_2(\eta-x)}d\eta$$

$$-\frac{T_3}{2}(L^2-1)\int_{x}^{\infty}\bar{v}_{,\eta}(\eta,0,p)e^{-\gamma_3(\eta-x)}d\eta$$

$$+\frac{T_3}{2}(L^2-1)\int_{-\infty}^{x}\bar{v}_{,\eta}(\eta,0,p)e^{\gamma_3(\eta-x)}d\eta$$

$$+\frac{t_2\gamma_2}{2}(L^2-1)\int_{x}^{\infty}\bar{\phi}(\eta,0,p)e^{-\gamma_2(\eta-x)}d\eta$$

$$-\frac{t_2\gamma_2}{2}(L^2-1)\int_{-\infty}^{x}\bar{\phi}(\eta,0,p)e^{\gamma_2(\eta-x)}d\eta$$

$$+\frac{t_3\gamma_3}{2}(L^2-1)\int_{x}^{\infty}\bar{\phi}(\eta,0,p)e^{-\gamma_3(\eta-x)}d\eta$$

$$-\frac{t_3\gamma_3}{2}(L^2-1)\int_{-\infty}^{x}\bar{\phi}(\eta,0,p)e^{\gamma_3(\eta-x)}d\eta$$

$$-\frac{p^2}{\gamma_1{}^2}\bar{v}(x,0,p)\ . \qquad (3.2.14)$$

3.3 Formulation of Integral Equations

The complete inversion of equations (3.2.7)-(3.2.9) and (3.2.14) is not necessary in this analysis, since the main interest here is in the determinations of the stress and the couple stress intensity factors. Instead, we need to obtain $t_{yy}(x,0,t)$ by applying the inverse transform to equation (3.2.14). The inverse

Fourier cosine transform for any point in the space is then taken and y is allowed to approach zero. Since $\bar{t}_{yy}(x,y,p)$ is continuous in y at y = 0, we can interchange the order of the limit process and integration in s. The inverse Fourier cosine transform which is defined by

$$\bar{f}(x,y,p) = \frac{2}{\pi} \int_0^\infty \hat{\bar{f}}(x,y,p) \cos(sy)\, ds \ , \qquad (3.3.1)$$

is performed on equation (3.2.14) for y = 0. The inverse Laplace transform is then taken to obtain the expression for t_{yy}. In view of the complexity of the functions $\gamma_i(s,p)$, i=1,2,3, it is not possible to perform the inversion of the Laplace transform without an appropriate approximation. We find it necessary to consider the case of large p, which corresponds to small t, based on the Tauberian theorems. The inverse Laplace transform is then taken by application of the Cagniard-Dehoop method and a convolution integral, that is, the expression for $\bar{t}_{yy}(x,y,p)$ obtained above, is changed into a recognizable Laplace transform by setting $\gamma_i|\eta-x| = pt$ (i = 1,2,3) in each double integral. Then, using the identity

$$\left[\overline{\frac{\partial}{\partial t} f*g(t)}\right] = p\, \bar{f}\, \bar{g} \ , \qquad (3.3.2)$$

where * denotes the convolution integral, we obtain

$t_{yy}(x,0,t) =$

$$\frac{\partial}{\partial t}\Big[\int_{-\infty}^{\infty}\int_{0}^{t} v_{,\eta}(\eta,0,\tau)H(t-\tau-|\eta-x|)\ M_1(t-\tau,\eta-x)d\tau d\eta$$
$$+\int_{-\infty}^{\infty}\int_{0}^{t} v_{,\eta}(\eta,0,\tau)H(t-\tau-|\eta-x|/A)\ M_2(t-\tau,\eta-x)d\tau d\eta$$
$$+\int_{-\infty}^{\infty}\int_{0}^{t} v_{,\eta}(\eta,0,\tau)H(t-\tau-|\eta-x|/\theta C_2)\ M_3(t-\tau,\eta-x)d\tau d\eta$$
$$+\int_{-\infty}^{\infty}\int_{0}^{t} \phi(\eta,0,\tau)H(t-\tau-|\eta-x|/A)\ M_4(t-\tau,\eta-x)d\tau d\eta$$
$$+\int_{-\infty}^{\infty}\int_{0}^{t} \phi(\eta,0,\tau)H(t-\tau-|\eta-x|/\theta C_2)\ M_5(t-\tau,\eta-x)d\tau d\eta\Big]\ , \tag{3.3.3}$$

where

$$M_1(\xi,\zeta) = \frac{2}{\pi C_2^{\,2}}\left[(1-L^2)\frac{\xi}{\zeta} - \frac{1}{2}\frac{\zeta}{\xi} - \frac{(L^2-1)^2}{2}\frac{\xi^3}{\zeta^3}\right][\xi^2-\zeta^2]^{-1/2}\ ,$$

$$M_2(\xi,\zeta) = \frac{(L^2-1)^2}{\pi C_2^{\,2}}\left[\frac{\xi}{\zeta^3}(\xi^2-\frac{\zeta^{2\frac{1}{2}}}{A^2}) + \frac{A^2\epsilon}{j}\frac{2+C^2/B^2}{(A^2/C_2^{\,2}-\theta^2)}\frac{1}{\zeta^3}\left\{\frac{\xi(\xi^2-\zeta^2/A^2)^{3/2}}{12} - \frac{\zeta^2\xi(\xi^2-\zeta^2/A^2)^{1/2}}{8A^2} + \frac{\zeta^4}{8A^4}\ln\frac{\xi+(\xi^2-\zeta^2/A^2)^{1/2}}{\zeta/A}\right\}\right]\ ,$$

$$M_3(\xi,\zeta) = -\frac{(L^2-1)^2}{\pi C_2^{\,2}}\frac{A^2\epsilon}{j}\frac{2+C^2/B^2}{(A^2/C_2^{\,2}-\theta^2)}\frac{1}{\zeta^3}\times\left[\frac{\xi(\xi^2-\zeta^2/\theta^2C_2^{\,2})^{3/2}}{12} - \frac{\zeta^2\xi(\xi^2-\zeta^2/\theta^2C_2^{\,2})^{1/2}}{8\theta^2C_2^{\,2}} + \frac{\zeta^4}{8(\theta C_2)^4}\ln\frac{\xi+(\xi^2-\zeta^2/\theta^2C_2^{\,2})^{1/2}}{\zeta/\theta C_2}\right]\ ,$$

$$M_4(\xi,\zeta) = \frac{(L^2-1)}{\pi}\frac{\theta^2C^2}{A^2-\theta^2C_2^{\,2}}\frac{\xi}{\zeta^3}(\xi^2-\zeta^2/A^2)^{1/2}\ ,$$

$$M_5(\xi,\varsigma) = -\frac{(L^2-1)}{\pi}\frac{\theta^2C^2}{A^2-\theta^2C_2{}^2}\frac{\xi}{\varsigma^3}(\xi^2-\varsigma^2/\theta^2C_2{}^2)^{\frac{1}{2}} \quad (3.3.4)$$

and H(t) is the Heaviside function. Equation (3.3.3) is rearranged in such a way that the terms with the Cauchy kernel $(\eta-x)^{-1}$ are extracted out and the terms with the kernel $(\eta-x)^{-3}$ in $M_i(i=1,2,..,5)$ are combined so that the strong singularities across $\eta=x$ are cancelled. Noting that the $v_{,\eta}(\eta,0,\tau)$ is equal to the macrorotation of the crack surface, $\omega(\eta,0,\tau)$, the following equation is obtained:

$$t_{yy}(x,0,t) = \frac{2(1-L^2)}{\pi C_2{}^2}\frac{\partial}{\partial t}J(x,t) \ , \quad (3.3.5)$$

where

$$\begin{aligned}
J(x,t) = &-\frac{(1-L^2)}{2}\int\int_{A_1-A_2}\omega(\eta,0,\tau)\frac{(t-\tau)^2}{(\eta-x)^3}\,d\tau d\eta \\
&+[1-(1-L^2)/4]\int\int_{A_1}\omega(\eta,0,\tau)\frac{1}{(\eta-x)}\,d\tau d\eta \\
&-\frac{(1-L^2)}{4A^2}\int\int_{A_2}\omega(\eta,0,\tau)\frac{1}{(\eta-x)}\,d\tau d\eta \\
&+\frac{1}{12}\frac{1-L^2}{2}\frac{A^2\epsilon}{j}\frac{2+C^2/B^2}{(A^2/C_2{}^2-\theta^2)}\int\int_{A_2-A_3}\Big\{ \\
&\omega(\eta,0,\tau)\frac{(t-\tau)^4}{(\eta-x)^3}\Big\}\,d\tau d\eta \\
&-\frac{1}{4}\frac{1-L^2}{2}\frac{A^2\epsilon}{j}\frac{2+C^2/B^2}{(A^2/C_2{}^2-\theta^2)}\int\int_{A_2}\Big\{ \\
&\frac{\omega(\eta,0,\tau)}{A^2}\frac{(t-\tau)^2}{(\eta-x)}\Big\}\,d\tau d\eta
\end{aligned}$$

$$+ \frac{1}{4}\frac{1-L^2}{2}\frac{A^2\epsilon}{j}\frac{2+C^2/B^2}{(A^2/C_2{}^2-\theta^2)}\int\int_{A_3}\Bigg\{ \frac{\omega(\eta,0,\tau)}{\theta^2C_2{}^2}\frac{(t-\tau)^2}{(\eta-x)}\Bigg\}\, d\tau d\eta$$

$$+ \int\int_{A_1}\omega(\eta,0,\tau)\ K_1(t-\tau,\eta-x)\times [(t-\tau)^2-(\eta-x)^2]^{-\frac{1}{2}}\, d\tau d\eta$$

$$+ \int\int_{A_2}\omega(\eta,0,\tau)\ K_2(t-\tau,\eta-x)\, d\tau d\eta$$

$$+ \int\int_{A_3}\omega(\eta,0,\tau)\ K_3(t-\tau,\eta-x)\, d\tau d\eta$$

$$- \frac{\pi}{2(1-L^2)}\int_{-1-a_-(t)}^{x}\omega(\eta,0,t)\, d\eta$$

$$- \frac{\theta^2C_2{}^2C^2}{2(A^2-\theta^2C_2{}^2)}\int\int_{A_2-A_3}\phi(\eta,0,\tau)\frac{(t-\tau)^2}{(\eta-x)^3}\, d\tau d\eta$$

$$+ \frac{\theta^2C_2{}^2C^2}{4A^2(A^2-\theta^2C_2{}^2)}\int\int_{A_2}\phi(\eta,0,\tau)\frac{1}{(\eta-x)}\, d\tau d\eta$$

$$+ \frac{\theta^2C_2{}^2C^2}{4\theta^2C_2{}^2(A^2-\theta^2C_2{}^2)}\int\int_{A_3}\phi(\eta,0,\tau)\frac{1}{(\eta-x)}\, d\tau d\eta$$

$$+ \int\int_{A_2}\phi(\eta,0,\tau)\ K_4(t-\tau,\eta-x)\, d\tau d\eta$$

$$+ \int\int_{A_3}\phi(\eta,0,\tau)\ K_5(t-\tau,\eta-x)\, d\tau d\eta\ , \qquad (3.3.6)$$

where

$$K_1(\xi,\varsigma) = \frac{\varsigma}{\xi}\left[\frac{1}{1+(1-\varsigma^2/\xi^2)^{\frac{1}{2}}} - \frac{1}{2(1-L^2)} - \frac{(1-L^2)}{8}\frac{3+\varsigma^2/\xi^2}{1+(1+0.5\varsigma^2/\xi^2)(1-\varsigma^2/\xi^2)^{\frac{1}{2}}}\right],$$

$$K_2(\xi,\varsigma) = -\frac{(1-L^2)}{4A^4}\frac{1}{\xi^2}\{1+q_1^{1/2}\}^{-2}$$

$$+\frac{1}{12}\frac{1-L^2}{2}\frac{A^2\epsilon}{j}\frac{2+C^2/B^2}{(A^2/C_2^2-\theta^2)}\frac{\xi}{A^4}\left[\{1.5+q_1^{1/2}\}^{-1}\right.$$

$$\left.-0.25\{1.5+q_1^{1/2}\}^{-1}\{1+q_1^{1/2}\}^{-2}\right]$$

$$+\frac{1}{8}\frac{1-L^2}{2}\frac{A^2\epsilon}{j}\frac{2+C^2/B^2}{(A^2/C_2^2-\theta^2)}\frac{\varsigma}{A^4}\left[\{1+q_1^{1/2}\}^{-1}\right.$$

$$\left.+\ln\frac{\xi+(\xi^2-\varsigma^2/A^2)^{1/2}}{\varsigma/A}\right],$$

$$K_3(\xi,\varsigma) = -\frac{1}{12}\frac{1-L^2}{2}\frac{A^2\epsilon}{j}\frac{2+C^2/B^2}{(A^2/C_2^2-\theta^2)}\frac{\xi}{\theta^4C_2^4}\times$$

$$\left[\{1.5+q_2^{1/2}\}^{-1}-0.25\{1.5+q_2^{1/2}\}^{-1}\{1+q_2^{1/2}\}^{-2}\right]$$

$$-\frac{1}{8}\frac{1-L^2}{2}\frac{A^2\epsilon}{j}\frac{2+C^2/B^2}{(A^2/C_2^2-\theta^2)}\frac{\varsigma}{\theta^4C_2^4}\left[\{1+q_2^{1/2}\}^{-1}\right.$$

$$\left.+\ln\frac{\xi+(\xi^2-\varsigma^2/A^2)^{1/2}}{\varsigma/\theta C_2}\right],$$

$$K_4(\xi,\varsigma) = \frac{\theta^2C_2^2C^2}{4A^4(A^2-\theta^2C_2^2)}\frac{\varsigma}{\xi^2}\{1+q_1^{1/2}\}^{-2},$$

$$K_5(\xi,\varsigma) = \frac{\theta^2C_2^2C^2}{4\theta^4C_2^4(A^2-\theta^2C_2^2)}\frac{\varsigma}{\xi^2}\{1+q_2^{1/2}\}^{-2},$$

$$q_1 = \left[1-\frac{1}{A^2}\frac{\varsigma^2}{\xi^2}\right],$$

$$q_2 = \left[1-\frac{1}{\theta^2C_2^2}\frac{\varsigma^2}{\xi^2}\right];$$

$$A_1 = \{(\eta,\tau)|\ 0<\tau<t-|\eta-x|,\ -1-a_-(\tau)<\eta<1+a_+(\tau)\},$$

$$A_2 = \{(\eta,\tau)|\ 0<\tau<t-|\eta-x|/A,\ -1-a_-(\tau)<\eta<1+a_+(\tau)\},$$

$$A_3 = \{(\eta,\tau)|\ 0<\tau<t-|\eta-x|/\theta C_2,$$
$$-1-a_-(\tau)<\eta<1+a_+(\tau)\} \ . \qquad (3.3.7)$$

Likewise, the transformed, normalized couple stress, $\hat{\bar{M}}_{yz}(x,s,p)$ is given by

$$\hat{\bar{M}}_{yz}(x,s,p) = j\theta^2[-\bar{\phi}(x,0,p) + s\tilde{\bar{\phi}}] \ . \qquad (3.3.8)$$

Substituting for $\tilde{\bar{\phi}}$ from equation (3.2.9) into equation (3.3.8), and integrating by parts, we obtain

$$\hat{\bar{M}}_{yz}(x,s,p) = -\frac{sW_3}{2}\int_x^\infty \bar{v}(\eta,0,p)e^{-\gamma_3(\eta-x)}d\eta$$
$$+\frac{sW_3}{2}\int_x^\infty \bar{v}(\eta,0,p)e^{\gamma_3(\eta-x)}d\eta$$
$$+\frac{s^2}{2\gamma_3{}^2}\int_x^\infty \bar{\phi}_{,\eta}(\eta,0,p)e^{-\gamma_3(\eta-x)}d\eta$$
$$-\frac{s^2}{2\gamma_3{}^2}\int_{-\infty}^x \bar{\phi}_{,\eta}(\eta,0,p)e^{\gamma_3(\eta-x)}d\eta \ . \qquad (3.3.9)$$

By following a method similar to that used for $t_{yy}(x,0,t)$, we obtain

$$M_{yz}(x,0,t) = \frac{j\theta^2}{\pi}\frac{\partial}{\partial t}J'(x,t) \qquad (3.3.10)$$

where

$$J'(x,t) = \int\int_{A_3}\phi_{,\eta}(\eta,0,\tau)\frac{1}{(\eta-x)}d\tau d\eta$$
$$+\int\int_{A_3}\phi_{,\eta}(\eta,0,\tau)\,K_6(t-\tau,\eta-x)\,d\tau d\eta$$
$$-(1-L^2)\frac{A^2\epsilon}{j}\frac{1}{C^2\theta^2}(2+C^2/B^2)\times$$
$$\left[\int\int_{A_3}v(\eta,0,\tau)\frac{(t-\tau)^2}{(\eta-x)^3}d\tau d\eta\right.$$

$$- \frac{1}{2\theta^2 C_2{}^2} \int\int_{A_3} v(\eta,0,\tau)\ \frac{1}{(\eta-x)}\ d\tau d\eta$$

$$+ \int\int_{A_3} v(\eta,0,\tau)\ K_7(t-\tau,\eta-x)\ d\tau d\eta \Big] \ , \qquad (3.3.11)$$

and where

$$K_6(\xi,\varsigma) = - \frac{\varsigma}{\theta^2 C_2{}^2 \xi^2}\ [1+q_2{}^{1/2}]^{-1} \ ,$$

$$K_7(\xi,\varsigma) = - \frac{\varsigma}{2\theta^4 C_2{}^4 \xi^2}\ [1+q_2{}^{1/2}]^{-2} \ . \qquad (3.3.12)$$

The η-integration in equations (3.3.6) and (3.3.11), which include the Cauchy kernels, is performed in the sense of the Cauchy principal value, if they do not exist in the sense of Riemann. Recalling that $t_{yy}(x,0,t)$ is given as a boundary condition on the crack surface, equation (3.3.5) can be viewed as an integro-differential equation for the unknown functions $\omega(\eta,0,\tau)$ and $\phi(\eta,0,\tau)$. Likewise, $M_{yz}(x,0,t)$ is given as a boundary condition on the crack surface and equation (3.3.10) can be viewed as another integro-differential equation for the unknown functions $v(\eta,0,\tau)$ and $\phi_{,\eta}(\eta,0,\tau)$. Moreover, $v(\eta,0,\tau)$ can be obtained from $\omega(\eta,0,\tau)$ and $\phi(\eta,0,\tau)$ from $\phi_{,\eta}(\eta,0,\tau)$. However, the evaluation of $\omega(\eta,0,\tau)$ and $\phi_{,\eta}(\eta,0,\tau)$ can only be carried out numerically since the equations are not analytically tractable. In order to facilitate the application of numerical techniques, equations (3.3.5)

and (3.3.10) are changed into integral equation form by integration with respect to time. Note that

$$\int_0^t t_{yy}(x,0,\tau)\, d\tau = \frac{2(1-L^2)}{\pi C_2{}^2} J(x,t) \ . \qquad (3.3.13)$$

For $|x| < 1$ the left hand side of the above equation is known, since $t_{yy}(x,0,\tau)$ is completely described on the time interval $(0,t)$. For $|x| > 1$ we split the time interval into $(0,t_c)$ and (t_c,t), where t_c is the time for the propagating crack tip to arrive at x, such that $x = 1+a_+(t_c)$ for $x > 1$ and $x = -1-a_-(t_c)$ for $x < -1$. Noting that t_{yy} is given for (t_c,t) and that

$$\int_0^{t_c} t_{yy}(x,0,\tau)\, d\tau = \frac{2(1-L^2)}{\pi C_2{}^2} J(x,t_c) \ ,$$

we obtain

$$\frac{2(1-L^2)}{\pi C_2{}^2} [J(x,t) - H(|x|-1)J(x,t_c)] = \begin{cases} \int_0^t t_{yy}(x,0,\tau)\, d\tau \ , & |x| < 1 \ , \\ \int_{t_c}^t t_{yy}(x,0,\tau)\, d\tau \ , & |x| > 1 \ . \end{cases} \qquad (3.3.14)$$

and

$$[J'(x,t) - H(|x|-1)J'(x,t_c)] = 0 \ . \qquad (3.3.15)$$

In equations (3.3.14) and (3.3.15), it is assumed that $t_c = 0$, if $|x| < 1$.

In order to evaluate $\omega(\eta,0,\tau)$ and $\phi_{,\eta}(\eta,0,\tau)$, present in equations (3.3.14) and (3.3.15), it is expedient to cast them in a form in which their singularities

are explicit. In view of previous analyses in the literature, two types of singularities can be expected. The first type is the square root singularity which arises at the crack tip, the proof of which can be found in Achenbach and Bazant [78] and Freund and Clifton [79]. The second type is the traveling logarithmic singularity located at the front of the Rayleigh wave, confirmed by Baker [31] and Thau and Lu [42], each of whom differentiated the normal displacement of the crack surface with respect to the coordinates of the crack propagation direction. Representation of this type of singularity for $\omega(\eta,0,\tau)$, however, makes the expression too cumbersome. Moreover, for a finite crack no information is available on the behavior of the traveling singularities after rediffraction of the cylindrical waves at the crack tips. For these reasons, the traveling singularities are neglected in the structure of ω. Also, it is known from the micropolar theory of elasticity that although ω and ϕ have similar properties, they are indeed independent of each other. From the static analyses of crack problems given above, the first type of singularity may be found; but no information is currently available for the second type of singularity. Therefore, ω and $\phi_{,\eta}$ are simply written as

$$\omega(\eta,0,\tau) = \frac{\Omega(\eta,\tau)}{[1+a_+(\tau)-\eta]^{1/2}[1+a_-(\tau)+\eta]^{1/2}} \qquad (3.3.16)$$

and

$$\phi_{,\eta}(\eta,0,\tau) = \frac{\Phi(\eta,\tau)}{[1+a_+(\tau)-\eta]^{1/2}[1+a_-(\tau)+\eta]^{1/2}} , \qquad (3.3.17)$$

where Ω and Φ are assumed to be bounded and continuous almost everywhere over the area, S, defined by $S = \{(\eta,\tau) | \tau \geq 0, -1-a_-(\tau) < \eta < 1+a_+(\tau)\}$. The functions Ω and Φ are zero if (η,τ) is not in S. Therefore, there is a jump discontinuity in Ω and Φ across the crack tip trajectories. In order to derive formulas for the stress and couple stress intensity factors, it is further assumed that Ω and Φ are analytic in the region S almost everywhere along the crack tip trajectories. Moreover, in the numerical integration process, Ω and Φ are treated as if they are bounded and continuous everywhere in S.

3.4 Stress and Couple Stress Intensity Factors

The dynamic stress intensity factor which represents the time-dependent strength of the square root singularity in t_{yy}, is defined in a manner analogous to the static stress intensity factor, that is

$$K_{ID}^{\pm}(t) = \lim_{\delta \to 0^+} \sqrt{2\pi\delta}\ t_{yy}(\pm 1 \pm a_{\pm}(t) \pm \delta, t) , \qquad (3.4.1)$$

where the upper and lower signs are, respectively, for the right and left crack tips. Note that $K_{ID}^{\pm}(t)$ is dimensionless because δ and t_{yy} are dimensionless. If the traction on the crack surface and the motion of the

crack tips are symmetric with respect to the y-axis, the stress intensity factors for the left and right crack tips are identical. In this case the ± sign will be deleted from the definition (3.4.1).

As mentioned earlier, one of the specific problems which is treated in this study prescribes uniform extension of the tips of the crack. The derivation of the stress intensity factor will be carried out only for this case. The formula obtained for this case will be extended to nonuniform propagation of the crack without a detailed proof. For uniform extension, equation (3.3.16) is written as

$$\omega(\eta,0,\tau) = \frac{\Omega(\eta,\tau)}{[(1+c\tau)^2-\eta^2]^{\frac{1}{2}}} . \qquad (3.4.2)$$

As stated in the previous section, $\Omega(\eta,\tau)$ is assumed to be analytic almost everywhere in S along $\eta = \pm 1 \pm c\tau$. Therefore, the expansion of $\Omega(\eta,\tau)$ into a Taylor series is possible in the neighborhood of almost all points on the lines. Now we consider the derivation of $K^{+}_{ID}(t)$. Redefining J(x,t) by substitution of (3.4.2) into (3.3.6) and using the definition (3.4.1), we get

$$K^{\pm}_{ID}(t) = \frac{2(1-L^2)}{{C_2}^2} \lim_{x\to(1+ct)^{+}} \sqrt{2\pi(x-1-ct)}\, \frac{\partial}{\partial t} J(x,t) , \qquad (3.4.3)$$

In order to evaluate the right-hand side of equation (3.4.3), we take a particular point (x,t) in the η-τ plane such that $x > 1+ct$ [see Figure 2(a), 2(b), 2(c)] and construct A_1, A_2 and A_3 by drawing the characteris-

tic lines. Then take a (N,T) coordinate system with the origin at (x,t) and a polar coordinate system (r,θ) where r is the distance from (x,t) and θ is measured counterclockwise from the N-axis. Then divide A_1 into A_{11} and A_{12} as shown in Figure 2(a). A_{11} is the little sector-like area generated by drawing a circle with its center at (x,t) and radius r_1. A_{11} includes the point (η_1,τ_1) which is the intersection of the two lines, $t-\tau = x-\eta$ and $\eta = 1+c\tau$. A_{12} is given by $A_1 - A_{11}$. Similarly, we divide A_2 into A_{21} and A_{22} as shown in Figure 2(b). A_{21} and A_{22} are divided by $r = r_2$ and A_{21} includes the point (η_2,τ_2) which is the intersection of $t-\tau = (x-\eta)/A$ and $\eta = 1+c\tau$. Likewise, we divide A_3 into A_{31} and A_{32} as shown in Figure 2(c). A_{31} and A_{32} are divided by $r = r_3$ and A_{31} includes the point (η_3,τ_3) which is the intersection of $t-\tau = (x-\eta)/\theta C_2$ and $\eta = 1+c\tau$. Now, we consider the contribution of each term in J(x,t) to $K_{ID}(t)$. Denote the contribution of i-th term by J_i. For i = 1,

$$J_1 = -\frac{(1-L^2)^2}{\pi C_2{}^2}\lim_{x\to(1+ct)^+}\sqrt{2\pi(x-1-ct)}\,\frac{\partial}{\partial t}\left[\iint_{A_1^-}-\iint_{A_2}\right]\frac{\Omega(\eta,\tau)}{\sqrt{(1+c\tau)^2-\eta^2}}\,\frac{(t-\tau)^2}{(\eta-x)^3}\,d\tau d\eta$$

$$= -\frac{(1-L^2)^2}{\pi C_2{}^2}\lim_{x\to(1+ct)^+}\sqrt{2\pi(x-1-ct)}\,\frac{\partial}{\partial t}\left[\iint_{A_{11}^+}\iint_{A_{12}}-\iint_{A_{21}^-}\iint_{A_{22}}\right]\frac{\Omega(\eta,\tau)}{\sqrt{(1+c\tau)^2-\eta^2}}\,\frac{(t-\tau)^2}{(\eta-x)^3}\,d\tau d\eta\ .$$

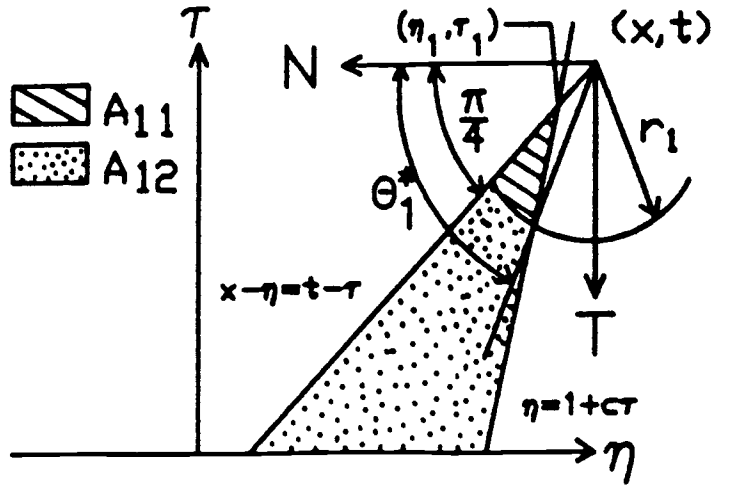

(a)

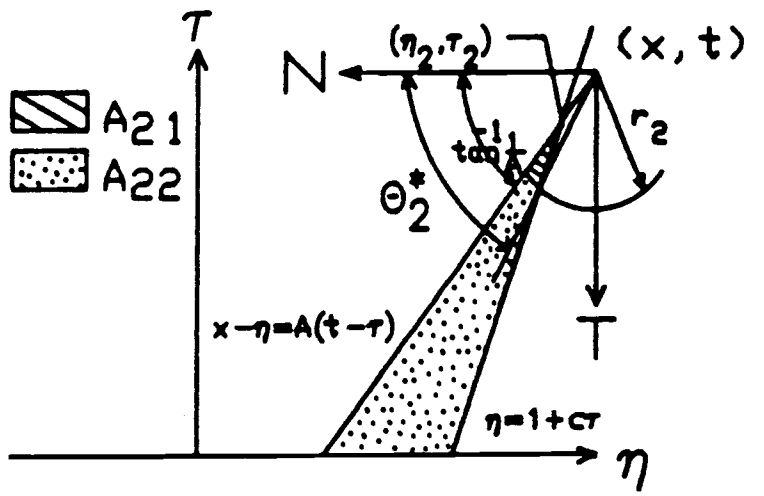

(b)

Figure 2. Division of the Area of Integration for Evaluation K_{ID}^{+}

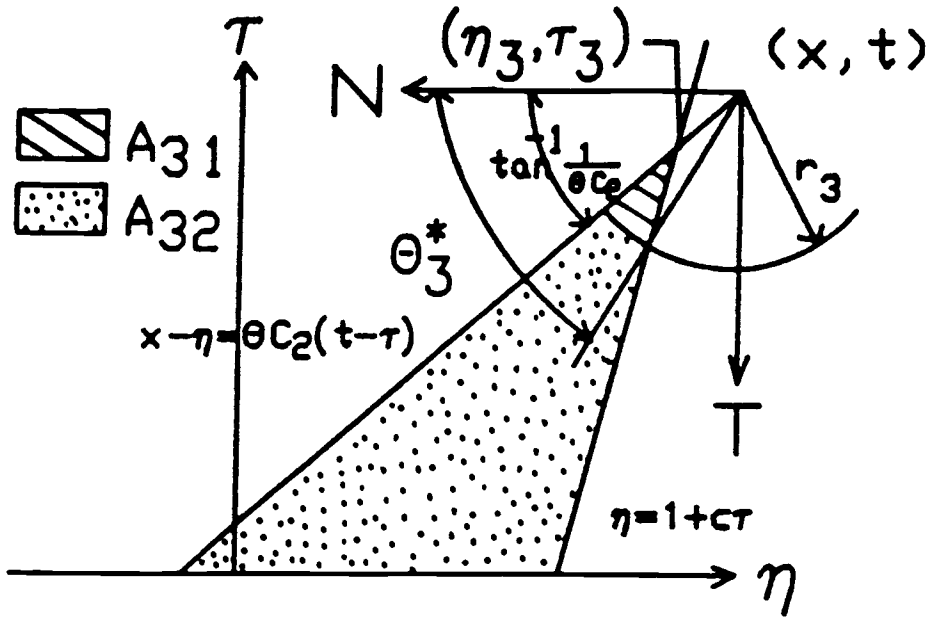

(c)

Figure 2 (continued).

It can be easily shown by direct differentiation of the integral that the second and fourth terms in the above equation are bounded and hence vanish after taking the limit. The contribution of the first and the third terms in J_1 are denoted by J_{11} and J_{13}, respectively. Using the polar coordinate system and expanding Ω into a Taylor series about (η_1,τ_1), J_{11} can be written as

$$J_{11} = \frac{(1-L^2)^2}{\pi C_2{}^2} \lim_{x\to(1+ct)^+} \sqrt{2\pi(x-1-ct)}\, \frac{\partial}{\partial t}\left[\frac{\Omega(\eta_1,\tau_1)}{\sqrt{1+c\tau_1+\eta_1}} \times \right.$$
$$\left. \int_{\pi/4}^{\theta_1^*} \frac{\sin^2\theta d\theta}{\cos^3\theta} \int_{r_0}^{r_1} \frac{dr}{\sqrt{1+c(t-r\sin\theta)-(x-r\cos\theta)}} + \Phi(x,t)\right]$$
$$= \frac{(1-L^2)^2}{\pi C_2{}^2} \lim_{x\to(1+ct)^+} \sqrt{2\pi(x-1-ct)}\, \frac{\Omega(1+ct,t)}{\sqrt{2(1+ct)}}$$
$$\int_{\pi/4}^{\theta_1^*} \frac{c\sin^2\theta d\theta}{\cos^3\theta(\cos\theta-c\sin\theta)\sqrt{r_1(\cos\theta-c\sin\theta)-(x-1-ct)}},$$

where $r_0 = (x-1-ct)/(\cos\theta-c\sin\theta)$ is the distance from (x,t) to $\eta = 1+c\tau$ along any fixed θ, θ_1^* is the angle at the intersection of $r = r_1$ and $\eta = 1+c\tau$, and $\Phi(x,t)$ is such that $\sqrt{x-1-ct}\ \Phi_{,t} \to 0$ as $x \to (1+ct)^+$. Introducing a new variable ξ defined by $\xi = x-r_1(\cos\theta-c\sin\theta)$ and denoting $\xi_1^* = x-r_1(\cos\theta_1^*-c\sin\theta_1^*) = 1+ct$, $\xi_0 = x - r_1[\cos(\pi/4) - c\sin(\pi/4)]$, we obtain

$$J_{11} = -\frac{(1-L^2)^2 c}{\pi C_2{}^2} \lim_{x\to(1+ct)^+} \sqrt{2\pi(x-1-ct)}\, \frac{\Omega(1+ct,t)}{\sqrt{2(1+ct)}} \times$$
$$\int_{\xi_0}^{\xi_1^*} \frac{\tan^2\theta(1+\tan^2\theta)d\xi}{(\tan\theta+c)(\xi-x)\sqrt{\xi_1^*-\xi}}.$$

The integral in the above equation is in the form of equation (29.3) in Muskhelishvili [80] (see Appendix C). Utilizing equation (29.5) of this reference, the above equation is reduced to

$$J_{11} = -\frac{(1-L^2)^2 c}{\pi C_2^2} \lim_{x\to(1+ct)^+} \sqrt{2\pi(x-1-ct)}\,\frac{\Omega(1+ct,t)}{\sqrt{2(1+ct)}} \times \left[-\frac{\tan^2\theta_1^*(1+\tan^2\theta_1^*)}{(\tan\theta_1^*+c)}\,\frac{\pi}{\sqrt{x-1-ct}} + \Psi(x,t)\right]$$

where $|\Psi(x,t)| < D/(x-1-ct)^{\alpha}$, D being a positive constant and $\alpha < 1/2$. Observing that

$$\lim_{x\to(1+ct)^+} \tan\theta_1^* = 1/c \ ,$$

we finally obtain

$$J_{11} = \frac{\pi^{1/2}(L^2-1)^2}{C^2C_2^2}\,\frac{\Omega(1+ct,t)}{\sqrt{1+ct}} \ .$$

Similarly, we can show that

$$J_{13} = -\frac{\pi^{1/2}(L^2-1)^2}{C^2C_2^2}\,\frac{\Omega(1+ct,t)}{\sqrt{1+ct}} \ .$$

Hence, $J_1 = J_{11} + J_{13} = 0$.

The evaluations of $J_2, J_3, \ldots, J_{15}$ are analogous and only the results are presented here:

$$J_2 = -\frac{2\pi^{1/2}(1-L^2)}{C^2C_2^2}\,[1-(1-L^2)/4]\,\frac{\Omega(1+ct,t)}{\sqrt{1+ct}} \ ,$$

$$J_3 = \frac{\pi^{1/2}(L^2-1)^2}{2A^2C_2^2}\,\frac{\Omega(1+ct,t)}{\sqrt{1+ct}} \ ,$$

$$J_4 = J_5 = J_6 = 0 \ ,$$

$$J_7 = -\frac{2(1-L^2)c^2\pi^{1/2}}{(1-c^2)^{1/2}C_2^{\,2}}\left[\frac{1}{1+(1-c^2)^{1/2}} - \frac{1}{2(1-L^2)} - \frac{(1-L^2)}{8}\,\frac{3+c^2}{[1+(1+0.5c^2)(1-c^2)^{1/2}]}\right],$$

$$J_8 = \frac{(L^2-1)^2\pi^{1/2}}{2A^2C_2^{\,2}}\,\frac{c^2}{A^2}\,[1+\sqrt{1-c^2/A^2}]^{-2},$$

and

$$J_9 = J_{10} = J_{11} = J_{12} = J_{13} = J_{14} = J_{15} = 0.$$

J_{10} vanishes since $v(-1-ct) = 0$ and $v(x,t) = 0$. Adding all the J's, the dynamic stress intensity factor becomes

$$K_{ID}^{+}(t) = f(A,C_2,c)\;\Omega(1+ct,t)/\sqrt{1+ct}\,, \qquad (3.4.4)$$

where

$$f(A,C_2,c) = -\frac{2(1-L^2)\pi^{1/2}}{C_2^{\,2}}\,[1-0.25(1-L^2)] + \frac{(L^2-1)^2\pi^{1/2}}{2A^2C_2^{\,2}} - \frac{2(1-L^2)c^2\pi^{1/2}}{(1-c^2)^{1/2}C_2^{\,2}}\left[\frac{1}{1+(1-c^2)^{1/2}} - \frac{1}{2(1-L^2)} - \frac{(1-L^2)}{8}\,\frac{3+c^2}{[1+(1+0.5c^2)(1-c^2)^{1/2}]}\right] + \frac{(L^2-1)^2\pi^{1/2}}{2A^2C_2^{\,2}}\,\frac{c^2}{A^2}\,[1+\sqrt{1-c^2/A^2}]^{-2}, \qquad (3.4.5)$$

for the right crack tip. In a similar manner, we obtain

$$K_{ID}^{-}(t) = -f(A,C_2,c)\;\Omega(-1-ct,t)/\sqrt{1+ct}\,, \qquad (3.4.6)$$

for the left crack tip. In the derivation of (3.4.4) and (3.4.6), c was assumed non-zero, but we can easily show that these equations are also valid for $c = 0$.

Recalling that $K_{ID}^{+}(t)$ was determined by considering the neighborhood of the point, (1+ct,t), in the η-τ plane, the applicability of equations (3.4.4) and (3.4.6) can be extended to general nonuniform propagation of the crack by replacing c with the instantaneous velocity $c_{\pm}(t)$ in $f(A,C_2,c)$ and replacing the argument of Ω and radical appropriately. In general, the following equation is then obtained:

$$K_{ID}^{\pm}(t) = \pm f[A,C_2,c_{\pm}(t)] \frac{\Omega[\pm 1 \pm a_{\pm}(t),t]}{[\{2+a_{-}(t)+a_{+}(t)\}/2]^{1/2}} . \tag{3.4.7}$$

Similarly, the dynamic couple stress intensity factor $K_{IM}^{\pm}(t)$ is defined by

$$K_{IM}^{\pm} = \lim_{\delta \to 0^{+}} \sqrt{2\pi\delta}/b \; M_{yz}(\pm 1 \pm a_{\pm}(t) \pm \delta, t) , \tag{3.4.8}$$

where the characteristic length b is given by

$$b^2 = \frac{\gamma}{2(2\mu+\kappa)}$$

and the upper and lower signs correspond, respectively, to the right and left crack tips.

For uniform extension, equation (3.3.17) is written as

$$\phi_{,\eta}(\eta,0,\tau) = \frac{\Phi(\eta,\tau)}{[(1+c\tau)^2-\eta^2]^{1/2}} . \tag{3.4.9}$$

Then, according to the definition,

$$K_{IM}^{+}(t) = g(\theta C_2,c)\; \Phi(1+ct,t)/\sqrt{1+ct} , \tag{3.4.10}$$

for the right crack tip and

$$g(\theta C_2,c) = -j\theta^2/b\pi \times$$

$$\left[1 - \frac{c^2}{\theta^2 C_2{}^2}\,[1+\{1-c^2/\theta^2 C_2{}^2\}^{1/2}]^{-1}\right] . \qquad (3.4.11)$$

In a similar manner, we obtain

$$K_{IM}^{-}(t) = -g(\theta C_2,c)\ \Phi(-1-ct,t)/\sqrt{1+ct}\ , \qquad (3.4.12)$$

for the left crack tip and in general,

$$K_{IM}^{\pm}(t) = \pm g[\theta C_2, c_{\pm}(t)]\ \frac{\Phi[\pm 1 \pm a_{\pm}(t),t]}{[\{2+a_{-}(t)+a_{+}(t)\}/2]^{1/2}} . \qquad (3.4.13)$$

In order to obtain $K_{ID}^{\pm}(t)$ and $K_{IM}^{\pm}(t)$, $\Omega[\pm 1 \pm a_{\pm}(t)]$ and $\Phi[\pm 1 \pm a_{\pm}(t)]$ are first obtained by solving the simultaneous integral equations, (3.3.14) and (3.3.15), numeri cally. Then $K_{ID}^{\pm}(t)$ and $K_{IM}^{\pm}(t)$ are computed by using equations (3.4.7) and (3.4.13).

3.5 Numerical Evaluation of the Integral Equation

3.5.1 Procedure for Numerical Scheme

As a numerical example, the diffraction of a uniform micropolar dilatational wave with a propagation vector normal to the crack plane for the cases of a stationary crack and a propagating crack with constant speed are investigated. The total wave field for a diffraction problem is determined by adding the incident wave field and the scattered wave field. For the purpose of determining the dynamic stress and couple stress intensity factors, only the scattered wave field must be considered. The boundary conditions (3.1.4)

and (3.1.5) for the scattered wave field are given, respectively, by

$$t_{yy}(x,0,t) = \begin{cases} -\sigma H(t) & |x| < 1 , \\ -\sigma H(t-\frac{|x|-1}{c}) & 1 < |x| < 1+ct \end{cases} \tag{3.5.1}$$

and

$$M_{yz}(x,0,t) = 0 ,$$

where σ is the uniform pressure on the crack surface, and $a(t) = a_+(t) = a_-(t)$.

The numerical procedure for the computation of integral equation (3.3.15) is outlined as follows: Introduce a new variable, defined by $\eta^* = \eta/[1+a(\tau)]$, and as a consequence the regions A_1, A_2, and A_3 are mapped, respectively, on to A_1^*, A_2^*, and A_3^* (see Fig. 2). Then, we divide A_1^*, A_2^*, and A_3^* into a set of horizontal strips of equal spacing with interval $\Delta\tau$. As previously noted, the logarithmic singularities are neglected and Ω^* and $\Phi^*{}_{,\eta^*}$ are approximated in each strip by

$$\Omega^*(\eta^*,\tau) = \sum_{j=1,3}^{2M-1} [a_{kj} + b_{kj}(\tau-\tau_k)] \, T_j(\eta^*) , \tag{3.5.2}$$

and

$$\Phi^*(\eta^*,\tau) \underset{j=2,4}{=} \sum^{2M} [c_{kj} + d_{kj}(\tau-\tau_k)] \, T_j(\eta^*) , \tag{3.5.3}$$

where $\Omega^*(\eta^*,\tau) = \Omega(\eta,\tau)$, $\Phi^*(\eta^*,\tau) = \Phi(\eta,\tau)$, $\tau_k \le \tau \le \tau_{k+1}$, and a_{kj}, b_{kj}, c_{kj} and d_{kj}, are constants, and T_j is the j^{th} order Chebyshev polynomial of the first kind. Note that only odd order polynomials are

included in the terms related to macrorotation, ω, and microrotation, ϕ, due to the antisymmetry of both rotations with respect to the y-axis for the problem under consideration, and that only even order polynomials are included in the terms related to displacement, v, in the y-direction and the gradient of microrotation, $\phi_{,\eta}$. Both $\tau_1 = 0$ and $a_{1j} = c_{1j} = 0$, are taken from the initial conditions. Then, from the continuity of Ω^* and Φ^* at $\tau = \tau_k$, we have $a_{kj} = a_{\ell j} + b_{\ell j}\Delta\tau$ and $c_{kj} = c_{\ell j} + d_{\ell j}\Delta\tau$, where $\ell = k-1$, and $\Delta\tau = \tau_k - \tau_{k-1}$. The problem is now reduced to the determination of b_{kj} and d_{kj} for each strip. In order to compute b_{ij} and $d_{ij}(\tau_1 < \tau < \tau_{i+1}=t)$, pick M values of x, which are the zeros of $T_{2M}(x/[1+a(t)])$ in $[0,1+a(t)]$, that is,

$$x_m = [1+a(t)] \cos\left(\frac{2m-1}{2M}\frac{\pi}{2}\right), \qquad (3.5.4)$$

where $m = 1,2,\ldots,M$. Then, substituting equation (3.5.2) into equation (3.3.14) and equation (3.5.3) into equation (3.3.15), the following $2M \times 2M$ simultaneous linear system of equations is obtained:

$$\sum_{k=1}^{i}\sum_{j=1,3}^{2M-1}[a_{kj}F_{j1k}(x_m,t) + b_{kj}F_{j2k}(x_m,t)]$$

$$+ \sum_{k=1}^{i}\sum_{j=2,4}^{2M}[c_{kj}G_{j1k}(x_m,t) + d_{kj}G_{j2k}(x_m,t)]$$

$$- \frac{\pi}{2(1-L^2)}\sum_{j=1,3}^{2M-1}[a_{kj} + b_{kj}(t-\tau_i)]\int_{-1}^{x_m} Q\, d\eta^*$$

$$- H(|x|-1) \sum_{k=1}^{k_c} \Big\{ \sum_{j=1,3}^{2M-1} [a_{kj}F_{j1k}(x_m,t_c) + b_{kj}F_{j2k}(x_m,t_c)] + \sum_{j=2,4}^{2M} [c_{kj}G_{j1k}(x_m,t_c) + d_{kj}G_{j2k}(x_m,t_c)] \Big\}$$

$$= \begin{cases} -t , & |x_m| < 1 , \\ -(t-t_c) , & |x_m| > 1 , \end{cases} \qquad (3.5.5)$$

and

$$\sum_{k=1}^{i} \sum_{j=1,3}^{2M-1} [a_{kj}D_{j1k}(x_m,t) + b_{kj}D_{j2k}(x_m,t)] + \sum_{k=1}^{i} \sum_{j=2,4}^{2M} [c_{kj}H_{j1k}(x_m,t) + d_{kj}H_{j2k}(x_m,t)]$$

$$- H(|x|-1) \sum_{k=1}^{k_c} \Big\{ \sum_{j=1,3}^{2M-1} [a_{kj}D_{j1k}(x_m,t_c) + b_{kj}D_{j2k}(x_m,t_c)] + \sum_{j=2,4}^{2M} [c_{kj}H_{j1k}(x_m,t_c) + d_{kj}H_{j2k}(x_m,t_c)] \Big\}$$

$$= 0 \qquad |x_m| < 1 \quad \text{or} \quad |x_m| > 1 , \qquad (3.5.6)$$

where $m = 1,2,\ldots,M$,

$$F_{j\ell k}(x_m,t)$$

$$= - \frac{(1-L^2)}{2} \int\int_{A^*_{1k}-A^*_{2k}} Q_f \frac{(t-\tau)^2}{[(1+c\tau)\eta^*-x_m]^3} \, d\tau d\eta^*$$

$$+ [1-(1-L^2)/4] \int\int_{A^*_{1k}} Q_f \frac{1}{[(1+c\tau)\eta^*-x_m]} \, d\tau d\eta^*$$

$$- \frac{(1-L^2)}{4A^2} \int\int_{A^*_{2k}} Q_f \frac{1}{[(1+c\tau)\eta^*-x_m]}\, d\tau d\eta^*$$

$$+ \frac{1-L^2}{24} \frac{A^2\epsilon}{j} \frac{2+C^2/B^2}{(A^2/C_2{}^2-\theta^2)}$$

$$\int\int_{A^*_{2k}-A^*_{3k}} Q_f \frac{(t-\tau)^4}{[(1+c\tau)\eta^*-x_m]^3}\, d\tau d\eta^*$$

$$- \frac{1-L^2}{8} \frac{A^2\epsilon}{j} \frac{2+C^2/B^2}{(A^2/C_2{}^2-\theta^2)}$$

$$\int\int_{A^*_{2k}} \frac{Q_f}{A^2} \frac{(t-\tau)^2}{[(1+c\tau)\eta^*-x_m]}\, d\tau d\eta^*$$

$$+ \frac{1-L^2}{8} \frac{A^2\epsilon}{j} \frac{2+C^2/B^2}{(A^2/C_2{}^2-\theta^2)}$$

$$\int\int_{A^*_{3k}} \frac{Q_f}{\theta^2 C_2{}^2} \frac{(t-\tau)^2}{[(1+c\tau)\eta^*-x_m]}\, d\tau d\eta^*$$

$$\int\int_{A^*_{1k}} Q_f \frac{K_1[t-\tau,(1+\gamma\tau^\circ\eta^*-x_m]}{\sqrt{(t-\tau)^2-[(1+c\tau)\eta^*-xm]^2}}\, d\tau d\eta^*$$

$$+ \int\int_{A^*_{2k}} Q_f\, K_2[t-\tau,(1+c\tau)\eta^*-x_m]\, d\tau d\eta^*$$

$$+ \int\int_{A^*_{3k}} Q_f\, K_3[t-\tau,(1+c\tau)\eta^*-x_m]\, d\tau d\eta^* \quad , \quad (3.5.7)$$

$$G_{j\ell k}(x_m,t) =$$

$$- \frac{\theta^2 C_2{}^2 C^2}{2(A^2-\theta^2 C_2{}^2)} \int\int_{A^*_{2k}-A^*_{3k}} \phi^* f_{\ell k}(\tau) \frac{(t-\tau)^2}{[(1+c\tau)\eta^*-x_m]^3}\, d\tau d\eta^*$$

$$+ \frac{\theta^2 C_2{}^2 C^2}{4A^2(A^2-\theta^2 C_2{}^2)} \iint_{A^*_{2k}} \phi^* \, f_{\ell k}(\tau) \frac{1}{[(1+c\tau)\eta^*-x_m]} \, d\tau d\eta^*$$

$$+ \frac{\theta^2 C_2{}^2 C^2}{4\theta^2 C_2{}^2(A^2-\theta^2 C_2{}^2)} \iint_{A^*_{3k}} \phi^* \, f_{\ell k}(\tau) \frac{1}{[(1+c\tau)\eta^*-x_m]} \, d\tau d\eta^*$$

$$+ \iint_{A^*_{2k}} \phi^* \, f_{\ell k}(\tau) \, K_4[t-\tau, (1+c\tau)\eta^*-x_m] \, d\tau d\eta^*$$

$$+ \iint_{A^*_{3k}} \phi^* \, f_{\ell k}(\tau) \, K_5[t-\tau, (1+c\tau)\eta^*-x_m] \, d\tau d\eta^* \, , \qquad (3.5.8)$$

$$D_{j\ell k}(x_m, t) = -(1-L^2) \frac{A^2 \epsilon}{jC^2\theta^2} (2+C^2/B^2) \times$$

$$\left[\iint_{A^*_{3k}} v^* \, f_{\ell k}(\tau) \frac{(t-\tau)^2}{[(1+c\tau)\eta^*-x_m]^3} d\tau d\eta^* \right.$$

$$- \frac{1}{2\theta^2 C_2{}^2} \iint_{A^*_{3k}} v^* \, f_{\ell k}(\tau) \frac{1}{[(1+c\tau)\eta^*-x_m]} \, d\tau d\eta^*$$

$$\left. + \iint_{A^*_{3k}} v^* \, f_{\ell k}(\tau) \, K_7[t-\tau, (1+c\tau)\eta^*-x_m] \, d\tau d\eta^* \right] , \qquad (3.5.9)$$

and

$$H_{j\ell k}(x_m, t) = \iint_{A^*_{3k}} Q_f \frac{1}{[(1+c\tau)\eta^*-x_m]} \, d\tau d\eta^*$$

$$+ \iint_{A^*_{3k}} Q_f \, K_6[t-\tau, (1+c\tau)\eta^*-x_m] \, d\tau d\eta^* \, , \qquad (3.5.10)$$

$$Q = \frac{T_j(\eta^*)}{\sqrt{1-\eta^{*2}}} \, , \qquad Q_f = \frac{T_j(\eta^*)}{\sqrt{1-\eta^{*2}}} \, f_{\ell k}(\tau) \, ,$$

$$\phi^* = \int \frac{T_j(\eta^*)}{\sqrt{1-\eta^{*2}}}\, d\eta^* \qquad (j=2,4,\ldots,2M) \ , \tag{3.5.11}$$

$$v^* = \int \frac{T_j(\eta^*)}{\sqrt{1-\eta^{*2}}}\, d\eta^* \qquad (j=1,3,\ldots,2M-1) \ ,$$

and

$$f_{1k}(\tau) = 1 \ , \qquad f_{2k}(\tau) = \tau-\tau_k \ .$$

The areas A^*_{1k}, A^*_{2k}, and A^*_{3k} of the k^{th} strip ($\tau_k \le \tau \le \tau_{k+1}$) are, respectively, associated with A^*_1, A^*_2, and A^*_3, and k_c is the number of the strip in which $\tau_{k_c} \le \tau_c \le \tau_{k_c+1}$. Equations (3.5.5) and (3.5.6) can be solved by use of a computer.

3.5.2 Numerical Integration

The double integrals $F_{j\ell k}$, $G_{j\ell k}$, $D_{j\ell k}$ and $H_{j\ell k}$, (3.5.6)-(3.5.10), are evaluated approximately by means of the Quadrature formulas of Gauss type [81]. For one-dimensional integrals, we have

$$\int_a^b w(\xi)\, f(\xi)\, d\xi \approx \sum_{i=1}^{n} w_i\, f(\xi_i) \ , \tag{3.5.12}$$

where $f(\xi)$ is a continuous function on [a,b], $w(\xi)$ is a weight function which is nonnegative on [a,b] and w_i's are the weights. Suppose that $\{P^*_i\}$ is a set of orthogonal polynomials over [a,b] with respect to $w(\xi)$ and ξ_i's are the roots of $P^*_n(\xi)$. The weights, w_i, are obtained by solving the following linear system:

$$\sum_{i=1}^{n} w_i\, f(\xi_i) = \int_a^b w(\xi)\, \xi^j\, d\xi$$

where $j = 0.1,2,\ldots,n-1$. Equation (3.5.12) is exact for polynomials of degree less than 2n-1. The Gram-Schmidt process is used for generating $P_i^*(\xi)$. First of all, we define

$$(f,g) = \int_a^b w(\xi)\, f(\xi)\, g(\xi)\, d\xi \ , \tag{3.5.13}$$

$$\|f\| = (f,f)^{1/2} \ , \tag{3.5.14}$$

$$I_n = \int_a^b w(\xi)\, \xi^n\, d\xi \ , \tag{3.5.15}$$

where (f,g) is the inner product of f and g over [a,b] with respect to $w(\xi)$, $\|f\|$ is the norm of f. Then we find

$$\begin{aligned}
&P_0(\xi) = 1 \ , \\
&\|P_0(\xi)\| = (1,1)^{1/2} = I_0^{1/2} \ , \\
&P_0^*(\xi) = 1/I_0^{1/2} \ , \\
&P_1(\xi) = \xi - (\xi,P_0^*)\, P_0^* = \xi - I_1/I_0 \ , \\
&\|P_1(\xi)\| = (\xi - I_1/I_0,\ \xi - I_1/I_0)^{1/2} \\
&\qquad = (I_2 - I_1^2/I_0)^{1/2}, \\
&P_1^*(\xi) = (\xi - I_1/I_0)/(I_2 - I_1^2/I_0)^{1/2} \ , \\
&P_2(\xi) = \xi^2 - (\xi^2,P_0^*)\, P_0^* - (\xi^2,P_1^*)\, P_1^*(\xi) \\
&\qquad = \xi^2 - \frac{I_0I_3-I_1I_2}{I_0I_2-I_1^2}\,\xi + \frac{I_1I_3-I_2^2}{I_0I_2-I_1^2} \ , \qquad (3.5.16) \\
&\ \vdots
\end{aligned}$$

where $\{P_i\}$ is the set of orthogonal polynomials from which $\{P_i^*\}$ is obtained by normalization. In order to

carry out the integration (3.5.6)-(3.5.10), we need to consider the following two cases according to the type of $w(\xi)$:

(i) $w(\xi) = 1$, $a=-1$, $b=1$:

In this case $\{P_i\}$ is a set of Legendre polynomials. The zeros, ξ_i, can be found in Stroud and Secrest [81]. If $[a,b] \neq [-1,1]$, we must transform the interval to $[-1,1]$ in order to use the tabulated values.

(ii) $w(\xi) = (1-\xi^2)^{-1/2}$:

In this case the zeros, ξ_i, can be found in Stroud and Secrest [81] or we can evaluate the ξ_i's and w_i's by using the following formula.

$$\xi_i = \cos\left(\frac{(2i-1)\pi}{2n}\right),$$

$$w_i = (1 - \xi_i^2)^{-1/2}, \qquad (3.5.17)$$

where $i = 1,2,\ldots,n$. Now, we go back to integration (3.5.6)-(3.5.10) and first, consider an approximate evaluation of each integral in the $F_{j\ell k}$, (3.5.6).

(1) First term:

Typical shapes of the area of integration, $A^*_{1k} - A^*_{2k}$, are shown in Figure 3(b). $A^*_{1k} - A^*_{2k}$, may include one or two areas located on both sides of $\eta = x_m$, depending upon the value of k and position of (x_m,t). If the area (right or left of $\eta = x_m$) includes the point where $|(1+c\tau)\eta^* - x_m| = t-\tau$ intersects $|\eta^*| = 1$, the area

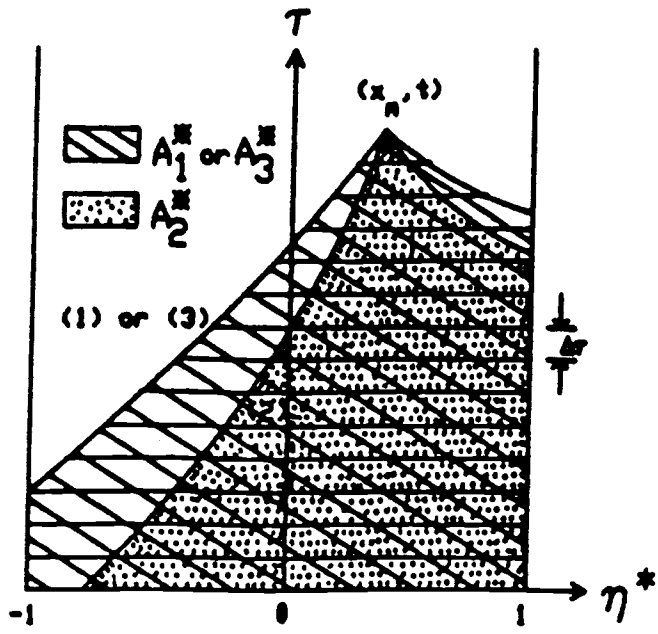

(a)

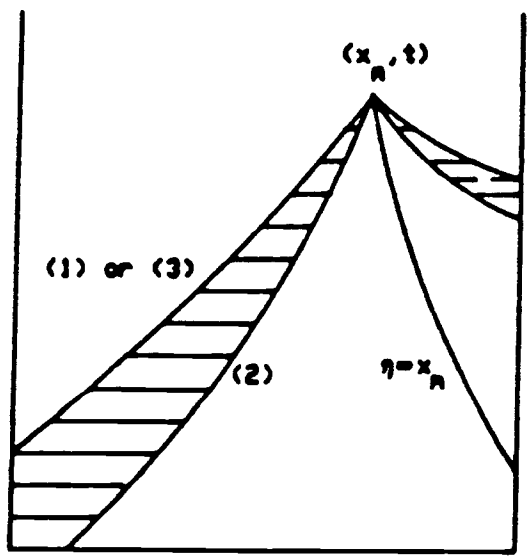

(b)

Figure 3. Subdivision of the Area of Integration for Numerical Integration:
(1) $|(1+c\tau)\eta^* - x_m| = t - \tau$;
(2) $|(1+c\tau)\eta^* - x_m| = A\,(t - \tau)$;
(3) $|(1+c\tau)\eta^* - x_m| = \theta C_2(t - \tau)$.

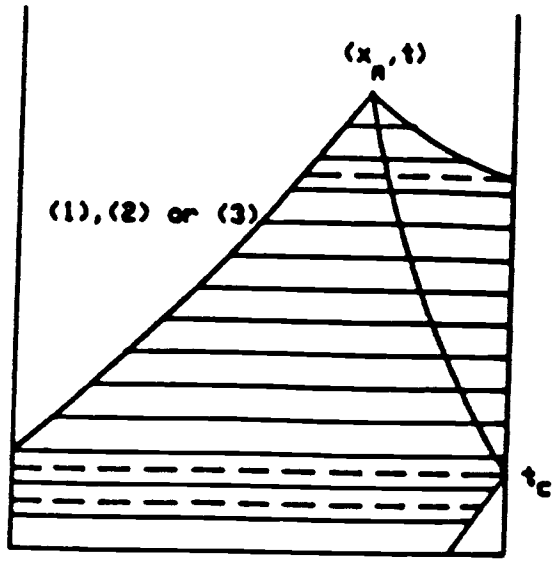

(c)

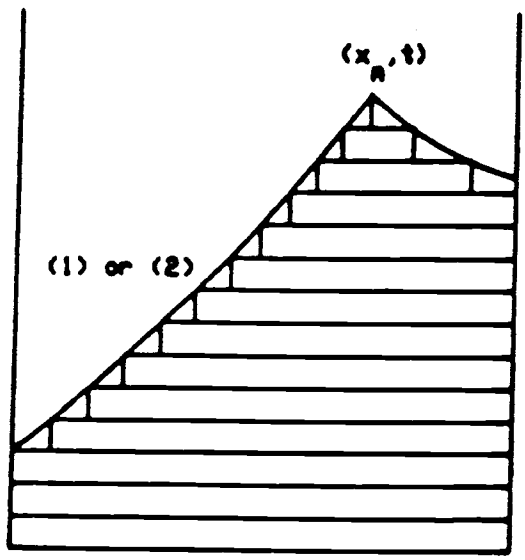

(d)

Figure 3 (continued).

is divided horizontally throughout that point. In order to approximate the integral over each piece of the area $A^*_{1k} - A^*_{2k}$, we first take two Gaussian points for the τ-integration, then for each value of τ, the integral of the η^*-integration is divided into subintervals. Over each subintervals, twenty Gaussian points are taken for the η^*-integration by using the equation (3.5.17). The approximate equation over each piece of the area is given by

$$\int\int Q_f \frac{(t-\tau)^2}{[(1+c\tau)\eta^*-x_m]^3}\, d\tau d\eta^*$$

$$\approx \sum_{p=1}^{2} \sum_{r=1}^{M_p} \sum_{q=1}^{20} w_p V_{prq} T_j(\eta^*_{prq}) \frac{f_{\ell k}(\tau_p)(t-\tau_p)^2}{[(1+c\tau_p)\eta^*_{prq}-x_m]^3} ,$$

where M_p is the number of subintervals for $\tau = \tau_p$, w_p and V_{prq} are weights for τ and η^*-integrations, respectively.

(2) Second and third terms:

The area of integration for these terms are A^*_{1k} and A^*_{2k}. Before performing integration the area of integration is divided horizontally, such that the right and left side boundaries are smooth for each divided area. An example of such a division of area is shown in Figure 3(c). Over each divided area, η^*-integration is performed numerically and then the τ-integration is performed numerically by use of equation (3.5.12) with n = 2. An outline of the integration process for these terms is given below:

Define:

$$U_j = \int\int_{A^*_{ik}} Q_f \frac{1}{[(1+c\tau)\eta^*-x_m]}\, d\tau d\eta^* = \sum_{n=1}^{N} B_{jn} ,$$

where

$$B_{jn} = \int_{\varsigma_n}^{\varsigma_{n+1}} \frac{f_{\ell k}(\varsigma)}{1+c\varsigma}\, d\varsigma \int_{\alpha(\varsigma)}^{\beta(\varsigma)} \frac{Q}{[\eta^*-x_m/(1+c\varsigma)]}\, d\eta^* ,$$

and $\tau_k = \varsigma_1 < \varsigma_2 < \cdots \varsigma_N < \varsigma_{N+1} = \tau_{k+1}$. N is the number of subareas in A^*_{ik} and B_{jn} is the interval over the n-th subarea. We generate a recurrence formula for the computation of U_j. First, we consider U_0. Define:

$$g(\varsigma) = \log \frac{[\sqrt{1-x_0^2}\,\sqrt{1-\alpha(\varsigma)^2} + 1-\alpha(\varsigma)x_0][\beta(\varsigma)-x_0]}{[\sqrt{1-x_0^2}\,\sqrt{1-\beta(\varsigma)^2} + 1-\beta(\varsigma)x_0][x_0-\alpha(\varsigma)]} ,$$

where $x_0 = x_m/(1+c\varsigma)$. Then, we have

$$B_{0n} = \int_{\varsigma_n}^{\varsigma_{n+1}} \frac{f_{\ell k}(\varsigma)g(\varsigma)}{\sqrt{(1+c\varsigma)^2-x_m^2}}\, d\varsigma ,$$

$$\approx \sum_{p=1}^{2} w_{np}\, S^0_{np} ,$$

where

$$S^0_{np} = \frac{f_{\ell k}(\varsigma_{np})g(\varsigma_{np})}{\sqrt{(1+c\varsigma_{np})^2-x_m^2}} .$$

U_0 is given by

$$U_0 \approx \sum_{n=1}^{N} \sum_{p=1}^{2} w_{np}\, S^0_{np} .$$

Second, we consider U_1. Using the relation

$$T_1(\eta^*) = \eta^* = \left(\eta^* - \frac{x_m}{1 + c\,\varsigma} \right) + \left(\frac{x_m}{1 + c\,\varsigma} \right) ,$$

we obtain

$$U_1 = \sum_{n=1}^{N} B_{1n} \approx \sum_{n=1}^{N} \sum_{p=1}^{2} w_{np} S_{np}^{1} ,$$

where

$$S_{np}^{1} = \frac{f_{\ell k}(\varsigma_{np}) a_1(\varsigma_{np})}{1 + c\ \varsigma_{np}} + \frac{x_m}{1+c\varsigma_{np}} S_{np}^{0}$$

and

$$a_1(\varsigma_{np}) = \sin^{-1}\beta(\varsigma_{np}) - \sin^{-1}\alpha(\varsigma_{np}) .$$

U_j for $j > 1$ is obtained similarly by using the relation

$$T_j(\eta^*) = 2\eta^*\ T_{j-1}(\eta^*) - T_{j-2}(\eta^*) .$$

The result is

$$U_j = \sum_{n=1}^{N} B_{jn} \approx \sum_{n=1}^{N} \sum_{p=1}^{2} w_{np} S_{np}^{j} , \qquad (3.5.19)$$

where

$$S_{np}^{j} = \frac{2f_{\ell k}(\varsigma_{np}) a_j(\varsigma_{np})}{1 + c\ \varsigma_{np}} + \frac{2\ x_m}{1+c\varsigma_{np}} S_{np}^{j-1} - S_{np}^{j-2}$$

and

$$a_j(\varsigma_{np}) = \{\sin[(j-1)\cos^{-1}\alpha(\varsigma_{np}) - \sin[(j-1)\cos^{-1}\beta(\varsigma_{np})]\}/(j-1) .$$

(3) Fourth term:

Division of the area of integration is analogous to (1). For each subarea shown in Figure 3(b), the following approximation formula is used:

$$\int\int Q_f \frac{(t-\tau)^4}{[(1+c\tau)\eta^* - x_m]^3}\, d\tau d\eta^*$$

$$\approx \sum_{p=1}^{2} \sum_{q=1}^{20} w_p v_{pq} T_j(\eta^*_{pq}) \frac{f_{\ell k}(\tau_p)(t-\tau_p)^4}{[(1+c\tau_p)\eta^*_{pq}-x_m]^3} \quad . \quad (3.5.20)$$

(4) Fifth and sixth terms:

Division of the area of integration is similar to (2). Since the integration procedure was explained in detail in (2), only the results of the approximation formula for each subarea shown in Figure 3(c) are presented here:

$$U_j = \sum_{n=1}^{N} B_{jn} \approx \sum_{n=1}^{N} \sum_{p=1}^{2} w_{np} S^j_{np} \quad , \quad (3.5.21)$$

where

$$S^j_{np} = \frac{2(t-\tau_p)^2 f_{\ell k}(\varsigma_{np}) a_j(\varsigma_{np})}{1 + c\,\varsigma_{np}} + \frac{2\,x_m}{1+c\varsigma_{np}} S^{j-1}_{np} - S^{j-2}_{np} \quad ,$$

and

$$a_j(\varsigma_{np}) = \{\sin[(j-1)\cos^{-1}\alpha(\varsigma_{np}) - \sin[(j-1)\cos^{-1}\beta(\varsigma_{np})]\}/(j-1) \quad .$$

(5) Seventh term:

The area of integration is divided into subareas as shown in Figure 3(d). For each subarea two Gaussian points are taken for the τ-integration. Then, for each value of τ, twenty Gaussian points are chosen for the η^*-integration. The integral over a rectangular area is approximated by

$$\int\int Q_f \frac{K_1[t-\tau,(1+c\tau)\eta^*-x_m]}{\sqrt{(t-\tau)^2-[(1+c\tau)\eta^*-x_m]^2}} \, d\tau d\eta^* \quad ,$$

$$\approx \sum_{p=1}^{2} \sum_{q=1}^{20} w_p V_{pq} T_j(\eta^*_{pq}) \frac{f_{\ell k}(\tau_p) K_1[t-\tau_p, (1+c\tau_p)\eta^*_{pq} - x_m]}{\sqrt{(t-\tau_p)^2 - [(1+c\tau_p)\eta^*_{pq} - xm]^2}} \tag{3.5.22}$$

where w_p and V_{pq} are weights for the τ- and η^*-integrations, respectively. In order to perform the integration over a triangular or trapezoidal area at the right or left end of A^*_{1k}, the integrable singularity $\{(t-\tau)^2 - [(1+c\tau_p)\eta^* - x_m]^2\}^{-1/2}$ is converted to the form (ii) by introducing a new variable $\xi = |(1+c\tau)\eta^* - x_m|/(t-\tau)$. We obtain the following result:

$$\int\int Q_f \frac{K_1[t-\tau, (1+c\tau)\eta^* - x_m]}{\sqrt{(t-\tau)^2 - [(1+c\tau)\eta^* - x_m]^2}} \, d\tau d\eta^*$$

$$= \int\int Q_f \frac{K_1[t-\tau, (1+c\tau)\eta^* - x_m]}{\sqrt{1-\xi^2}} \frac{1}{\xi \pm c\eta^*} \, d\xi d\eta^*$$

$$\approx \sum_{p=1}^{20} \sum_{q=1}^{20} w_p V_{pq} T_j(\eta^*_p) \frac{f_{\ell k}(\tau_{pq}) K_1[t-\tau_{pq}, (1+c\tau_{pq})\eta^*_p - x_m]}{(\xi_{pq} \pm c\eta^*_p)}, \tag{3.5.23}$$

where

$$\tau_{pq} = \frac{\xi_{pq} t - |\eta^*_p - x_m|}{\xi_{pq} \pm c\,\eta^*_p},$$

and the ± signs are for the right and left triangular or trapezoidal areas, respectively.

(7) Eighth and Ninth terms:

Division of the area of integration is similar to (6). For each subarea shown in Figure 3(d), the fol-

lowing approximation formulas are used for the eighth term

$$\int\int Q_f\, K_2[t-\tau,(1+c\tau)\eta^*-x_m]\, d\tau d\eta^* ,$$

$$\approx \sum_{p=1}^{2}\sum_{q=1}^{20} w_p V_{pq} T_j(\eta^*_{pq}) f_{\ell k}(\tau_p)\, K_2[t-\tau_p,(1+c\tau_p)\eta^*_{pq}-x_m] , \tag{3.5.24}$$

and for the ninth term

$$\int\int Q_f\, K_3[t-\tau,(1+c\tau)\eta^*-x_m]\, d\tau d\eta^* ,$$

$$\approx \sum_{p=1}^{2}\sum_{q=1}^{20} w_p V_{pq} T_j(\eta^*_{pq}) f_{\ell k}(\tau_p)\, K_3[t-\tau_p,(1+c\tau_p)\eta^*_{pq}-x_m] . \tag{3.5.25}$$

In order to obtain $G_{j\ell k}$ in equation (3.5.8), we need the expression for ϕ^*, which is obtained by the use of equation (3.5.11), evaluating it from the second order Chebyshev polynomial since ϕ^* should be an odd order polynomial due to anti-symmetry properties about the x- and y-axes and zero at $\eta^* = 0$ and 1. The result is as follows:

$$\phi^* = -\eta^* \sqrt{1-\eta^{*2}} \qquad (j = 2)$$

$$\phi^* = -\eta^* \sqrt{1-\eta^{*2}}\,(2\eta^{*2}-1) \qquad (j = 4)$$

$$\phi^* = -\eta^* \sqrt{1-\eta^{*2}}\,[(16/3)\eta^{*4}-(16/3)\eta^{*2}+1] \qquad (j = 6)$$

$$\vdots$$

The integrations of (3.5.8) for the first three integrals are similar to the integration in (2) above. According to the area of integration, the η^*-integration is performed analytically over each

divided area and the τ-integration is then performed numerically. The last two integrals can be evaluated by using a method similar to (7).

The integration of equation (3.5.10) requires an expression for v^*, which can be obtained by the use of equation (3.5.11). The result is as follows:

$$v^* = -\sqrt{1-\eta^{*2}} \qquad (j = 1)$$

$$v^* = -\sqrt{1-\eta^{*2}}\,[(4/3)\eta^{*2}-(1/3)] \qquad (j = 3)$$

$$v^* = -\sqrt{1-\eta^{*2}}\,[3.2\eta^{*4}-2.4\eta^{*2}+0.2] \qquad (j = 5)$$

•
•
•

The first and second integrations of (3.5.9) are similar to (1) and (2), respectively. According to the area of integration, the η^*-integration is performed analytically over each divided area and then the τ-integration is performed numerically. The third integration can be evaluated by using a formula similar to (7).

For the integration of (3.5.10), evaluations can be obtained by the same methods used in (2) and (7).

CHAPTER 4

RESULTS AND DISCUSSION

The dynamic stress and the couple stress intensity factors given by equations (3.4.3) and (3.4.9) can be rewritten as follows:

$$K^*_{ID}(t) = \frac{\sqrt{\pi}C_2{}^2}{2(1-L^2)}\, f(A,C_2,c)\ \Omega^*(1,t)\ , \qquad (4.1)$$

$$K^*_{IM}(t) = \frac{\pi b}{j\theta^2}\, g(j\theta^2,c)\ \Phi^*(1,t)\ . \qquad (4.2)$$

where equation (4.1) is obtained by dividing equation (3.4.3) by $\sigma\sqrt{\pi}$ and equation (4.2) is obtained by multiplying equation (3.4.9) by $\pi b/j\theta^2$ and utilizing the boundary condition $t_{yy}(x,0,\tau) = -\sigma = -2(1-L^2)/\pi C_2{}^2$ (see equation (3.3.13)).

The coefficients of the unknown functions, $\Omega^*(\eta^*,t)$ and $\Phi^*(\eta^*,t)$, were computed by solving the simultaneous two-dimensional singular integral equations (3.5.5) and (3.5.6), from which the normalized dynamic stress and couple stress intensity factors were obtained by use of equations (4.1) and (4.2). The micropolar coupling factor, N, is a measure of the strength of influence of the micropolar effects and is defined by

$$N = \left(\frac{\kappa}{2(\mu+\kappa)}\right)^{1/2}. \tag{4.3}$$

As a consequence of thermodynamic restrictions of the material moduli, $\mu \geq 0$, $\kappa \geq 0$, we find that the range of N to be $0 \leq N \leq 1/\sqrt{2}$. When N is equal to zero, the micropolar effect is absent and we obtain the case of a classical elastic solid. When N is equal to $1/\sqrt{2}$, the micropolar effect becomes maximum.

The numerical results of the stress intensity factors for N = 0., 0.2, 0.4, and 0.6, when b = 0.95 and j = 3×10^{-4} in^2 [74], in the case of a stationary crack, are shown in Figure 4, and are compared with the work of Baker [31]. Equation (3.3.5) for stress involves ω and ϕ, and equation (3.3.10) for couple stress involves both the displacement transverse to the crack surface and the gradient of microrotation. The classical solution for the corresponding problem has also been obtained as a special case of our micropolar solution by dropping the micropolar moduli in equation (3.5.5) and following the same numerical procedure. The corresponding curve is depicted in Figure 4, along with the asymptotic solution of Baker [31], for the purpose of comparison. Our result is found to be within 5 percent of that of Baker. The figure shows that the micropolar stress intensity factors increase with the micropolar coupling factor. The numerical results of the couple stress intensity factors for N = 0.2, 0.4, and 0.6,

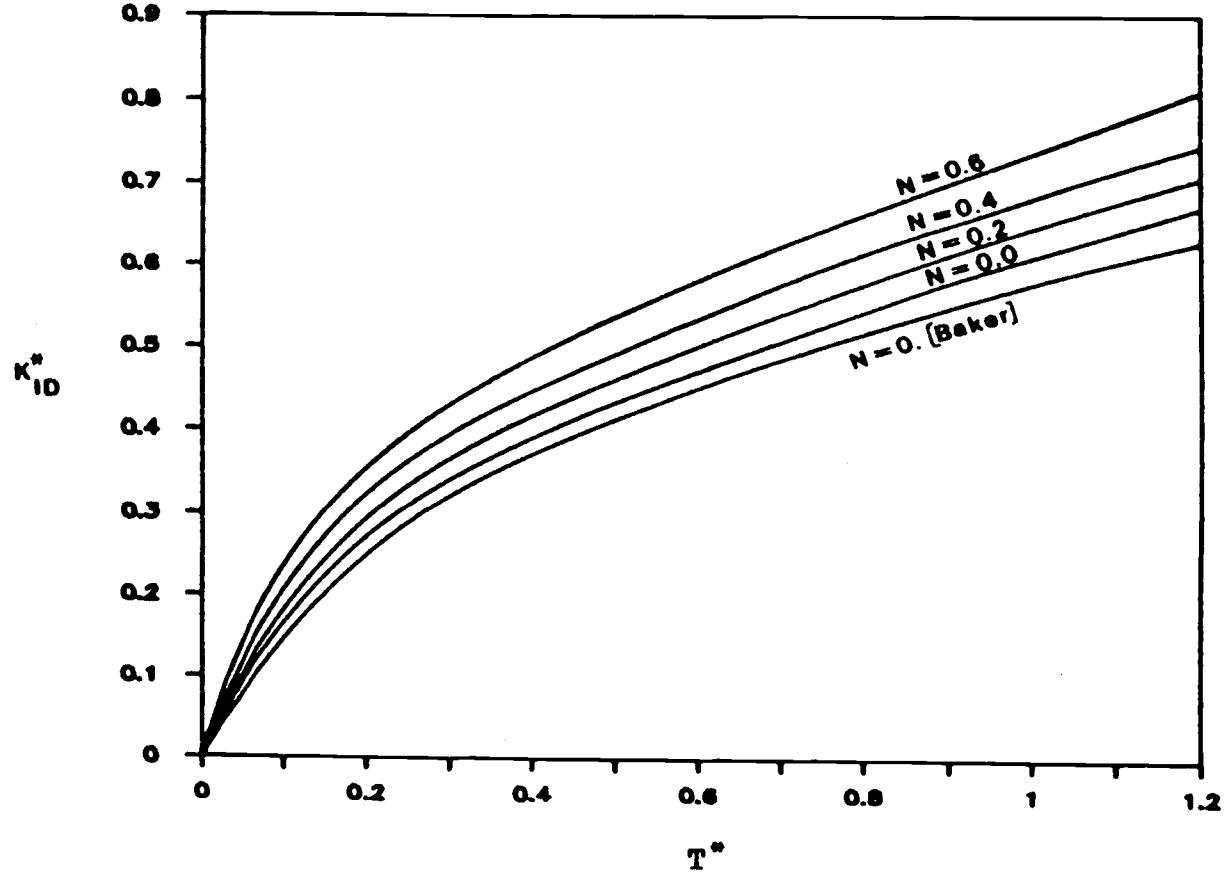

Figure 4. Normalized Dynamic Stress Intensity Factor of a Stationary Crack for Various Coupling Factors (ν=0.292)
T^* = Normalized Time = $t[(\lambda+2\mu+\kappa)/\rho]^{1/2}$

when b = 0.95 and j = 3×10^{-4} in^2 [74], in the case of a stationary crack, are shown in Figure 5. It also shows that the couple stress intensity factors increase with the micropolar coupling factor. A preliminary calculation of both the stress and the couple stress intensity factors for $0 \leq t \leq 2$, showed that the stress intensity factor increases monotonically with time, but the couple stress intensity factor begins to oscillate at t = 1.4. Hence, the physically acceptable time range of the solution is thought to be between t = 0. and t = 1.2.

The characteristic length, b, is a material property on which the influence of couple stresses are strongly dependent. If the ratio of the smallest dimension of a body to b is large, the theory indicates that the effect of couple stresses is negligible. However, when there are large strain gradients and a dimension of a body approaches b, couple stresses may produce effects of appreciable magnitude. The numerical results of the stress intensity factors for b = 0.2, 0.5, and 0.95 when N = 0.2 and j = 3×10^{-4} in^2, in the case of a stationary crack, are shown in Figure 6. The numerical computations for b = 0.5 and 0.95 in Figure 6, produced nearly coincident results. The numerical results of the couple stress intensity factors for b = 0.2, 0.5, and 0.95 when N = 0.2 and j = 3 $\times$

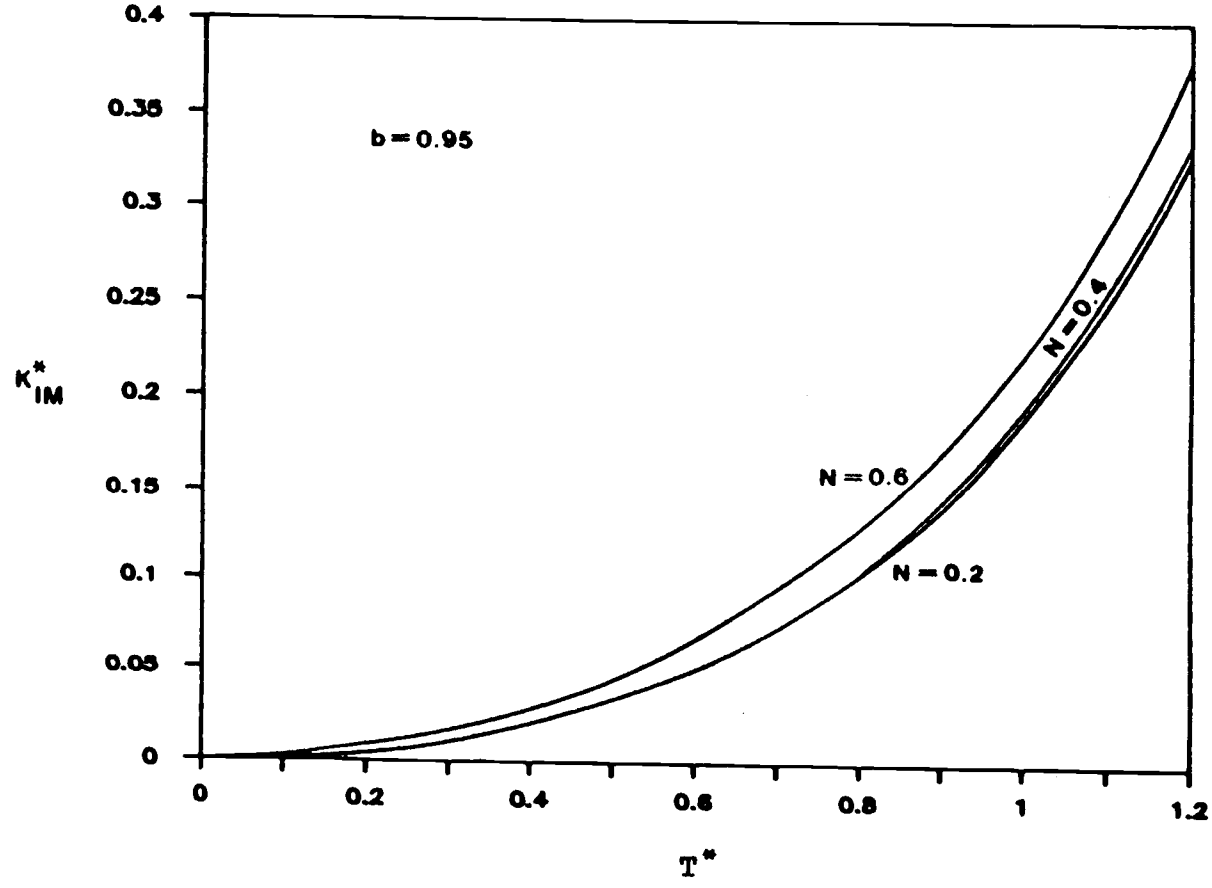

Figure 5. Normalized Dynamic Couple Stress Intensity Factor of a Stationary Crack for Various Coupling Factors (ν=0.292)
T^* = Normalized Time = $t[(\lambda+2\mu+\kappa)/\rho]^{1/2}$

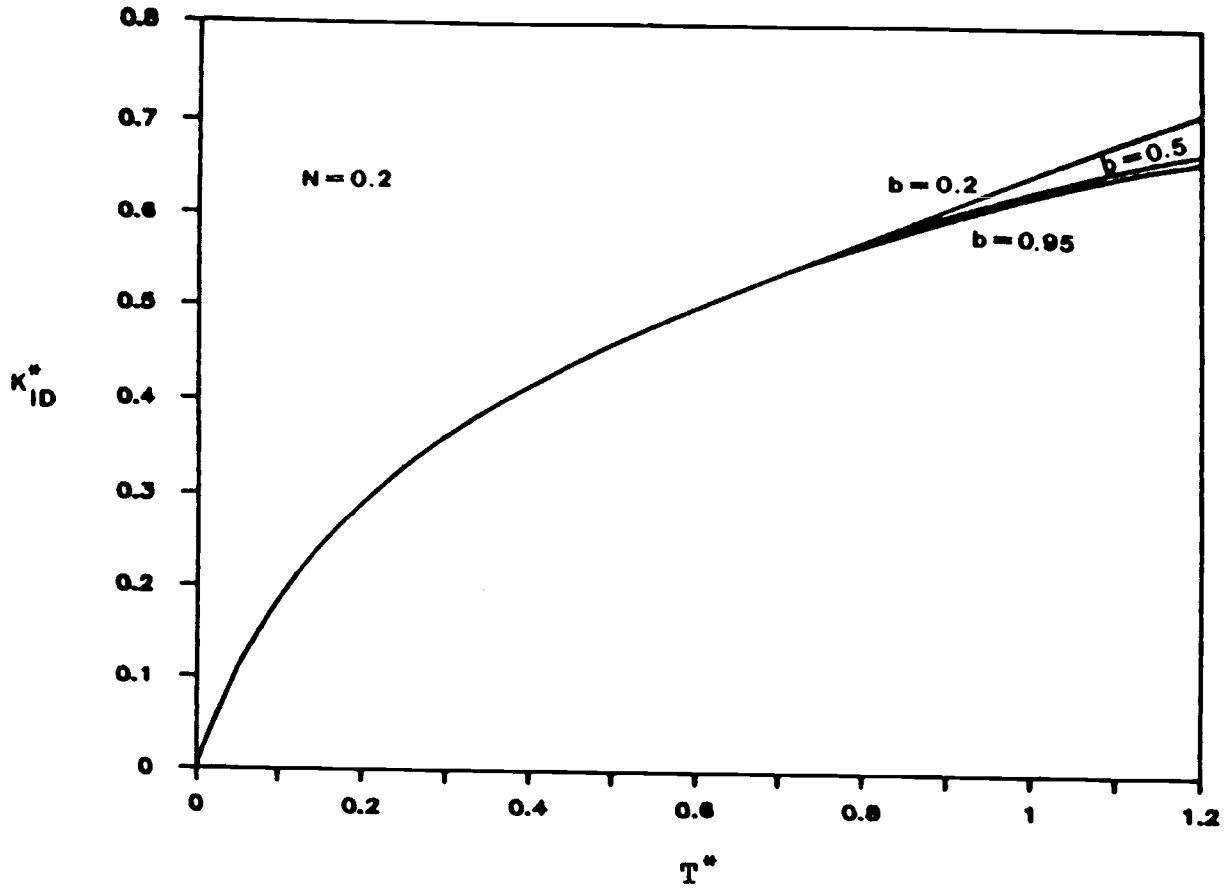

Figure 6. Normalized Dynamic Stress Intensity Factor of a Stationary Crack for Various Characteristic Lengths (ν=0.292)
T^* = Normalized Time = $t[(\lambda+2\mu+\kappa)/\rho]^{1/2}$

10^{-4} in^2, in the case of a stationary crack, are shown in Figure 7. The results show that the couple stress intensity factors decrease as the characteristic length increases.

The numerical results of the stress intensity factors for N = 0, and 0.2, when b = 0.5 and c = 0.2A, where A is given by (3.2.6) and j = 3×10^{-4} in^2, are shown in Figure 8, and are compared with the work of Baker. It is found from Figure 8 that the micropolar dynamic stress intensity factor is greater than the classical dynamic stress intensity factor in the case of c = 0.2A. It is also found that the micropolar stress intensity factor of a propagating crack with c = 0.2A is smaller than that of a stationary crack. The numerical results of the couple stress intensity factors for N = 0, and 0.2, when b = 0.5 and c = 0.2A and j = 3×10^{-4} in^2, are shown in Figure 9. It is found from Figure 9 that the micropolar dynamic couple stress intensity factor of the stationary crack is greater than that of the propagating crack with c = 0.2A. Since the numerical results for the range c greater than 0.2A are found to oscillate rapidly, it is hard to evaluate the precise value at the crack tips. Hence, we calculated and showed only one case of a propagating crack with a constant speed.

In summary, the micropolar stress intensity factor is always greater than the classical stress intensity

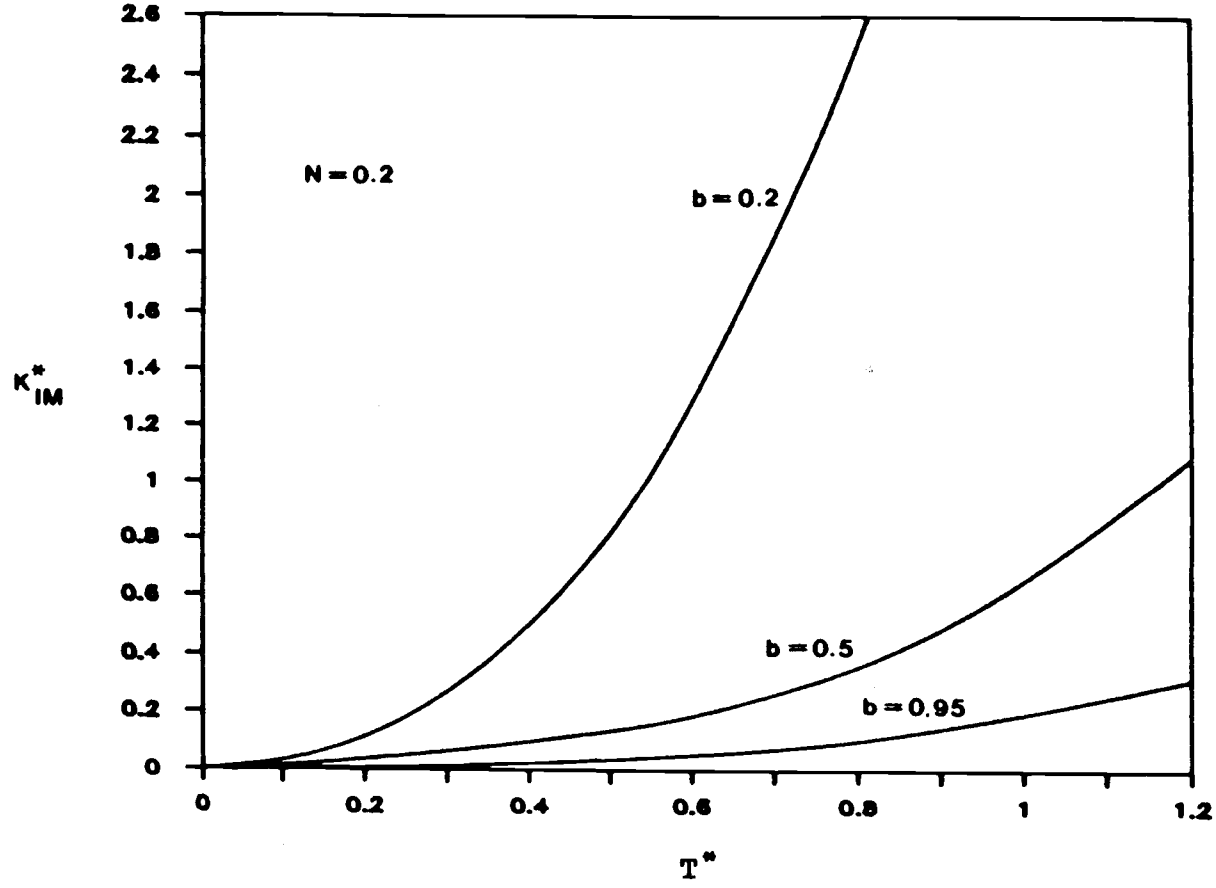

Figure 7. Normalized Dynamic Couple Stress Intensity Factor of a Stationary Crack for Various Characteristic Lengths (ν=0.292)
T^* = Normalized Time = $t[(\lambda+2\mu+\kappa)/\rho]^{1/2}$

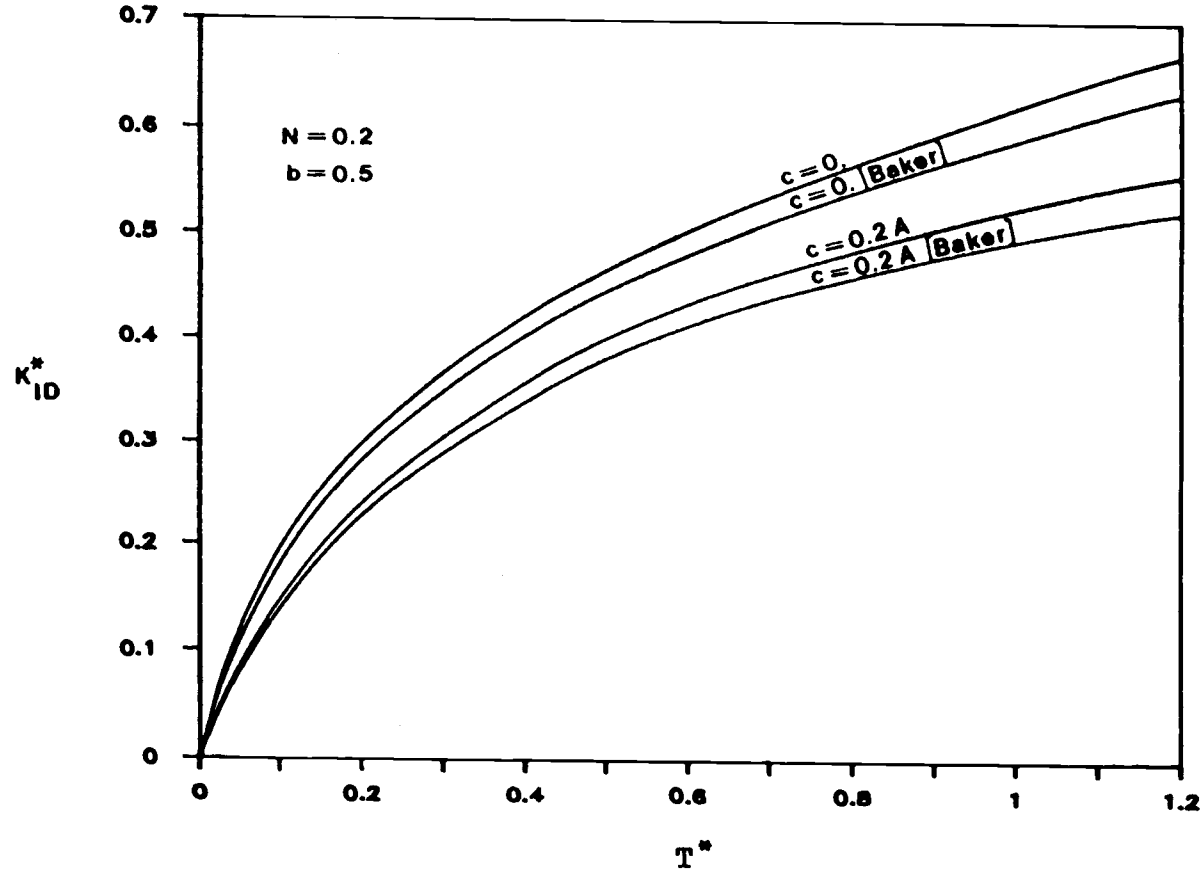

Figure 8. Normalized Dynamic Stress Intensity Factor of a Propagating Crack with Constant Speed for a Coupling Factor (ν=0.292)
T^* = Normalized Time = $t[(\lambda+2\mu+\kappa)/\rho]^{1/2}$

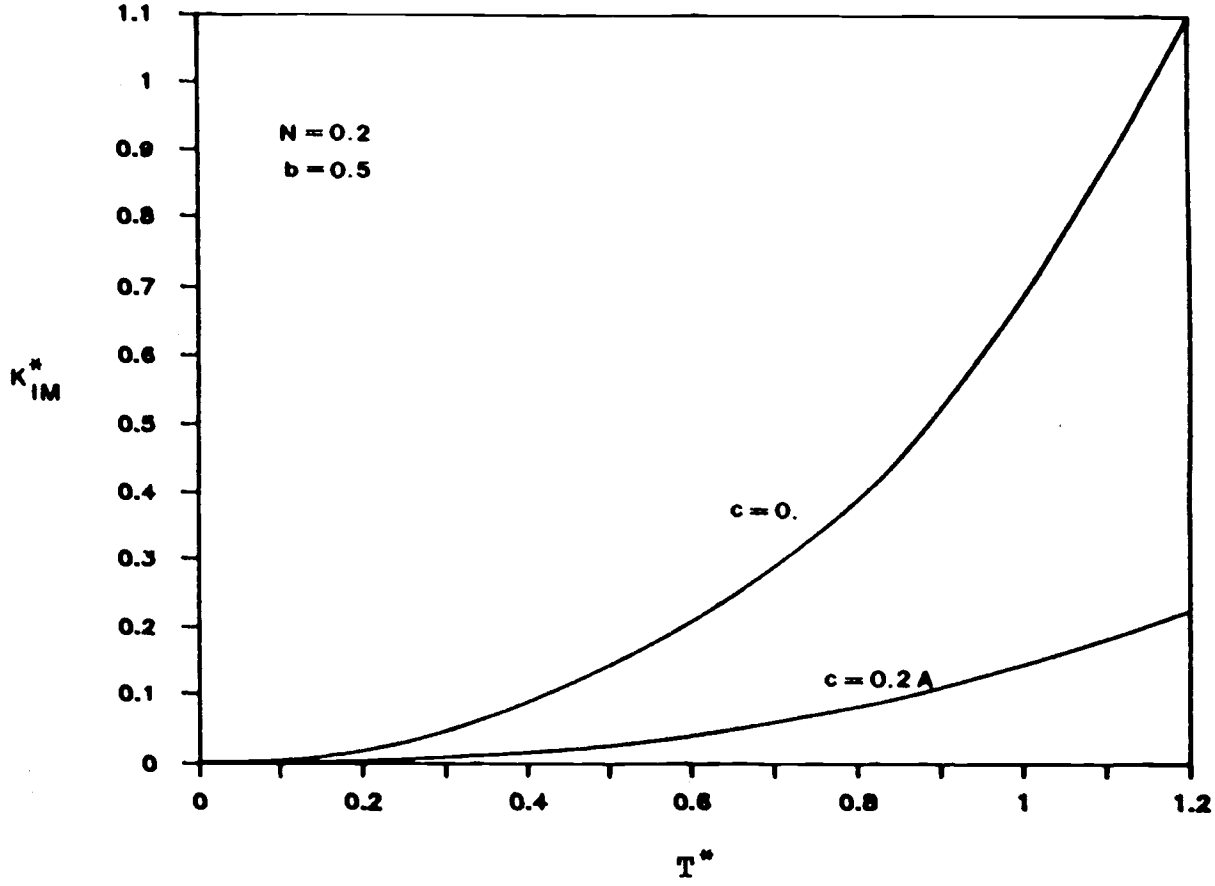

Figure 9. Normalized Dynamic Couple Stress Intensity Factor of a Propagating Crack with Constant Speed for a Coupling Factor (ν=0.292)
T^* = Normalized Time = $t[(\lambda+2\mu+\kappa)/\rho]^{1/2}$

factor for both a stationary crack and a propagating crack at constant speed. The characteristic length does not significantly affect the micropolar stress intensity factor, while it does affect the couple stress intensity factor, as long as the characteristic length for a finite crack is of the order of half of the crack length. The Laplace transform inversion procedure, based on the Tauberian theorems, that was used to make the present problem tractable, restricted the analysis to the normalized time of about $t = 1.2$, as mentioned earlier. Although the solution for the times when the stress and couple stress intensity factors reached their maximum values was not obtained, useful information about the dynamic crack propagation process has been found to emerge from our solution concerning the behavior of the micropolar stress and couple stress distributions, the microrotation field and microinertia.

CHAPTER 5

CLOSURE

The method developed in this study provides important information on the behaviors of the dynamic stress intensity factor and the dynamic couple stress intensity factor of a propagating finite crack in a micropolar elastic solid. In the formulation of the problem, the velocities of the crack tips are not restricted except that they are non-negative and bounded by the Rayleigh wave speed. Also, the normal traction on the crack surface may be an arbitrary function of time and space. Therefore the method is applicable to a crack problem in which the crack may accelerate and decelerate under a static or dynamic loading condition. The method is also applicable to non-symmetric propagation of a crack. The results found in this study are summarized as follows:

1) The stress intensity factors of a stationary crack increase with the micropolar coupling factor.

2) The couple stress intensity factors of a stationary crack increase with the micropolar coupling factor.
3) The stress intensity factors of a stationary crack increase as the characteristic length decreases, though not significantly.
4) The couple stress intensity factors of a stationary crack increase as the characteristic length decreases.
5) The stress intensity factor of a propagating crack with a constant speed is smaller than that of a stationary crack.
6) The stress intensity factor of a propagating crack with a constant speed in a micropolar elastic solid is greater than that in a classical elastic solid.
7) The couple stress intensity factor of a propagating crack with a constant speed is smaller than that of a stationary crack.

The present work could be extended by developing suitable techniques for both the Laplace and the Fourier inversions. Also, suitable experimental devices for measuring the micropolar elastic moduli should be designed.

REFERENCES

[1] R. D. MINDLIN and H. F. TIERSTEN, Effects of Couple Stresses in Linear Elasticity, *Arch. Rat. Mech. Analysis* 11, 415 (1962).

[2] A. C. ERINGEN and E. S. SUHUBI, Non-linear Theory of Microelastic Solids, *Int. J. Eng. Sci.* 2, 189 (1964); 389 (1964).

[3] W. VOIGT, Theoretische Studien über die Elastizitätsverhältnisse der Kristalle,Quarter-Point Singular Elements Revisited, *Abh. Ges. Wiss. Göttingen* 34, (1887).

[4] P. Duhem, Le Potential Thermodynamicque et la Pression Hydrostatique, *Ann. Ecole Norm.* 10, 187 (1893).

[5] E. and F. COSSERAT, Theorie des Corps Deformables, Hermann, Paris (1909).

[6] W. GÜNTHER, Zur Statik und Kinematik des Cosserat-Kontinuums, *Abh. Braunschweig. Wiss. Ges.* 10, 195 (1958).

[7] G. GRIOLI, Elasticita Asimmetrica, *Ann. Mat. Pura Appl., Ser. 4.* 50, 389 (1960).

[8] C. TRUESDELL and R. A. TOUPIN, The Cassical Field Theories, *Encyclopedia of Physics*, volume III/1, Springer Verlag, Berlin (1960).

[9] E. V. KUVSHINSKI and E. L. AERO, Continuum Theory of Non-Symmetric Elasticity (in Russian), *Physics of Solids* 5, 2591 (1963).

[10] H. SCHAEFE, Versuch einer Elastizitatstheorie des Zweidimensionalenebenen Cosserat-Kontinuuma, *Misz. Angew. Math. Festschrift Tollmien*, Akademie Verlag, Berlin (1962).

[11] R. A. TOUPIN, Theories of Elasticity with Couple Stresses, *Arch. Rat. Mech. Analysis* 17, 85 (1964).

[12] A. C. ERINGEN, Nonlinear Theory of Continuous Media, McGraw-Hill, New York (1962)

[13] A. C. ERINGEN, Linear Theory of Micropolar Elasticity, *Jour. Math. Mech.* 15, 909 (1966).

[14] A. C. ERINGEN, Mechanics of Micromorphic Continua, *Mechanics of Generalized Media* ed. by E. Kröner, Springer-Verlag, Berlin (1968).

[15] A. C. ERINGEN, Linear Theory of Nonlocal Elasticity and Dispersion of Plane Waves, *Int. J. Eng. Sci.* 10, 425, (1972).

[16] F. ERDOGAN, Crack Propagation Theories, Fracture ed. by H. Liebowitz, volume 2, Academic Press, 497 (1968).

[17] J. D. ACHENBACH, Dynamic Effects in Brittle Fracture, *Mechanics Today* ed. by S. Nemat-Nasser, volume 1, Pergamon Press, 1 (1972).

[18] J. D. ACHENBACH, Wave Propagation, Elastodynamics Stress Singularities, and Fracture, *Proceedings of the 14th IUTAM Congress* ed. by W. T. Koiter, North-Holland Publishing Co., 71 (1976).

[19] L. B. FREUND, The Analysis of Elastodynamic Crack Tip Stress Fields, *Mechanics Today* ed. by S. Nemat-Nasser, volume 3, Pergamon Press, 55 (1976).

[20] L. B. FREUND, Dynamic Crack Propagation, *The Mechanics of Fracture* ed. by F. Erdogan, ASME AMD-volume 19, American Society of Mechanical Engineers, 105 (1976).

[21] V. S. GOEL, The Mechanism of Fracture, Conference Proceedings, American Society for Metals (1985).

[22] M. L. WILLIAMS and W. G. KNAUSS, Dynamic Fracture, Martinus Nijhoff Publishers (1985).

[23] E. H. YOFFE, The moving Griffith crack, *Phil. Mag.* 42, 739 (1951).

[24] J. W. CRAGGS, On the propagation of a crack in an elastic brittle materials, *Jour. Mech. Phys. Solids* 8, 66 (1960).

[25] K. RAVI-CHANDAR and W. G. KNAUSS, An Experimental Investigation into Dynamic Fracture: IV. On the Interaction of Stress Waves with Propagating Cracks, *Int. J. Fract.* 26, 193 (1984).

[26] J. R. RICE, Mathematical Analysis in the Mechanics of Fracture, *Fracture* ed. by H. Liebowitz, volume 2, Academic Press, 191 (1968).

[27] A. JAHANSHAHI, A Diffraction Problem and Crack Propagation, *Jour. of Appiled Mech.* 34, 100 (1967).

[28] E. P. CHEN and G. C. SIH, Running crack in an incident wave field, *Int. J. Solids Struct.* 9, 897 (1973).

[29] G. C. SIH and J. F. LOEBER, Wave propagation in an elastic solid with a line of discontinuity or finite crack, *Quart. Appl. Math.* 27, 193 (1969).

[30] K. B. BROBERG, The propagation of a Brittle Crack, *Arkiv Fysik*, 18, 159 (1960).

[31] B. R. BAKER, Dynamic stresses created by a moving crack, *Jour. Appl. Mech.* 29, 449 (1962).

[32] J. W. CRAGGS, Fracture Criteria for Use in Continuum Mechanics, *Fracture of Solids*, ed. by D. C. Drucker and J. F. Gilman, Interscience Publisher, 51 (1963).

[33] B. V. KOSTROV, Unsteady Propagation of Longitudinal Shear Cracks, *Applied Math. and Mech. (English Transaction of PMM)*, 30, 1042 (1966)

[34] J. D. ESHELBY, The Elastic Field of a Crack Extending Non-uniformly under General Anti-plane Loading, Journal of the Mechanics and Physics of Solids, 17, 177 (1969)

[35] J. D. Achenbach, Extension of a Crack by a Shear Wave, *Zeitschrift fur Angewandte Mathematik und Physik*, 21, 887 (1970).

[36] J. D. ACHENBACH and R. NUISMER, Fracture Generated by a Dilatational Wave, *Int. J. Fract. Mech.*, 7, 77 (1971).

[37] L. B. FREUND, Crack propagation in an elastic solid subjected to general loading-I. Non-uniform rate of extension, *Jour. Mech. Phys. Solid* 20, 129 (1972).

[38] L. B. FREUND, Crack propagation in an elastic solid subjected to general loading-II. Non-uniform rate of extension, *Jour. Mech. Phys. Solid* 20, 141 (1972).

[39] L. B. FREUND, Crack propagation in an elastic solid subjected to general loading-III. Non-uniform rate of extension, *Jour. Mech. Phys. Solid* 21, 47 (1973).

[40] B. V. KOSTROV, On the Crack Propagation with Variable Velocity, *Int. J. Fract.*, 11, 47 (1975)

[41] E. B. GLENNIE and J. R. WILLIS, An Examination of the Effects of Some Idealized Models of Fracture on Accelerating Cracks, *Jour. Mech. Phys. Solid* 19, 11 (1971).

[42] S. A. THAU and T. H. LU, Transient stress intensity factors for a finite crack in an elastic solid caused by a dilatational wave, *Int. J. Solids. Struct.* 7, 731 (1971).

[43] G. C. SIH, G. T. EMBLEY, and R. S. RAVERA, Impact Response of a Finite Crack in Plane Extension, *Int. J. Solids. Struct.* 8, 977 (1972).

[44] G. P. CHEREPANOV and E. F. AFANAS'EV, Some Dynamic Problems of The Theory of Elasticity, *Int. J. Eng. Sci.* 12, 665 (1974).

[45] K. S. KIM, Dynamic propagation of a finite crack, *Int. J. Solids. Struct.* 15, 685 (1979).

[46] C. ATKINSON and J. D. ESHELBY, The Flow of Energy into the Tip of a Moving Crack, *Int. J. Fract. Mech.* 4, 3 (1968).

[47] C. C. MA and P. BURGERS, Dynamic Mode-I and Mode-II Crack Kinking Including Delay Time Effects, *Int. J. Solids Struct.* 23, 7, 897 (1987).

[48] A. CHATTOPADHYAY and U. BANDYOPADHYAY, Propagation of a Crack Due to Shear Waves in a Medium of Monoclinic Type, *Acta Mechanica* 71, 145 (1988).

[49] M. F. KANNINEN, *Numerical Methods in Fracture Mechanics*, D. R. J. Owen and A. R. Luxmoore, eds. Pineridge Press, 612 (1978).

[50] A. S. KOBAYASHI, A. F. EMERY and S. MALL, Dynamic-Finite-Element and Dynamic-Photoelastic Analyses of Two Fracturing Homalite-100 Plates, *Experimental Mechanics* 16, 321 (1976).

[51] S. MALL and J. LUZ, Use of Eight-Node Element for Fast Fracture Problems, *Int. J. Fract.* 16, R33 (1980).

[52] L. HODULAK, A. S. KOBAYASHI, A. F. EMERY, A Critical Examination of a Numerical Fracture Dynamic Code, *Fracture Mechanics*, P. C. Paris, ed. ASTM STP 700, 174 (1980).

[53] Z. BAZANT, J. L. GLAZIK Jr. and J. D. ACHENBACH, Elastodynamic Fields Near Running Cracks by Finite Elements, *Computers and Structures* 8, 193 (1978).

[54] K. KISHIMOTO, S. AOKI and M. SAKATA, Computer Simulation of Fast Crack Propagation in Brittle Material, *Int. J. Fract.* 16, 3 (1980).

[55] T. NISHIOKA and S. N. ATLURY, Numerical Modeling of Dynamic Crack Propagation in Finite Bodies by Moving Singular Elements, *Jour. Applied Mech.* 47, 570, (1980).

[56] S. N. ATLURY and T. NISHIOKA, Numerical Studies in Dynamic Fracture Mechanics, *Int. J. Fract.* 27, 245 (1985).

[57] K. KISHIMOTO, S. AOKI and M. SAKATA, On the Path Independent Integral-J, *Eng. Fract. Mech.* 13, 841 (1980).

[58] K. KISHIMOTO, S. AOKI and M. SAKATA, Dynamic Stress Intensity Factor Using J-Integral and Finite Element Method, *Eng. Fract. Mech.* 13, 387 (1980).

[59] L. BANKS-SILLS, Quarter-Point Singular Elements Revisited, *Int. J. Fract.* 34, R63 (1987).

[60] P. N. KALONI and T. ARIMAN, Stress Concentrations in Micropolar Elasticity, *Z. angew. Math. Phys.* 18, 136 (1967).

[61] R. D. MINDLIN, Influence of Couple Stresses on Stress Concentrations, *Exp. Mech.* 3, 1, (1963).

[62] S, C. COWIN, An Incorrect Inequality in Micropolar Elasticity Theory. *Jour. Appl. Math. and Physics. (ZAMP)* 21, 494, (1970).

[63] E. STERNBERG and R. MUKI, The Effect of Couple-Stresses on the Stress Concentration Around a Crack, *Int. J. Solids Struct.* 3, 69 (1967).

[64] C. ATKINSON and F. G. LEPPINGTON, The Effect of Couple Stresses on the Tip of a Crack, *Int. J. Solids Struct.* 13, 1103 (1977).

[65] J. and V. SLADEK, The Effect of Couple Stresses on the Stress Field around a Penny-Shaped Crack, *Int. J. Fract.* 25, 109, (1984).

[66] H. S. PAUL and K. SRIDHARAN, The Penny-Shaped Crack Problem in MIcropolar Elasticity, *Int. J. Eng. Sci.* 18, 651, (1980).

[67] R. S. DHALIWAL and S. M. KHAN, The Axisymmetric Boussinesq Problem for a Semi-Space in Micropolar Theory, *Int. J. Eng. Sci.* 14, 769 (1976).

[68] H. S. PAUL and K. SRIDHARAN, The Problem of a Griffith Crack in MIcropolar Elasticity, *Int. J. Eng. Sci.* 19, 563, (1981).

[69] B. CARBONARO and R. RUSSO, On Some Classical Theorems in Micropolar Elasticity, *Int. J. Eng. Sci.* 23, 119, (1985).

[70] T. M. MAI, Some Path Independent Integrals for Micropolar Media, *Int. J. solids Struct.* 22, 729, (1986).

[71] J. R. RICE, A path Independent Integral and Approximate Analysis of Strain Concentration by Notches and Cracks, *Jour. Appl. Mech.* 35, (1968).

[72] J. P. JARIC and E. S. SUHUBI, Griffith Criterion for Brittle Fracture in Micropolar Continuum, *Int. J. Eng. Sci.* 26, 495, (1988).

[73] K. M. RAO, Longitudinal Wave Propagation in a Micropolar Wave Guide, *Int. J. Eng. Sci.* 26, 135, (1988).

[74] R. D. GAUTHIER and W. E. JAHSMAN, A Quest for Micropolar Elastic Constant-II, Second Polish-Swedish Symposium in Micropolar Solids, Stockholm (1979)

[75] J. F. C. YANG and R. S. LAKES, Transient Study of Couple Stress Effects in Compact Bone: Torsion, *Jour. Biomech. Eng.* 103, 275, (1981).

[76] D. J. MALCOLM, Orthogonal Fibre Composites as Micromorphic Materials, *Int. J. Eng. Sci.* 20, 1111, (1982).

[77] A. C. ERINGEN, Continuum Physic volume 4-Polar and Nonlocal Field Theories, Academic Press, New York (1976).

[78] J. D. ACHENBACH and Z. P. BAZANT, Elastodynamic near-tip stress and displacement fields for rapidly propagating cracks in orthotropic materials, *Jour. Appl. Mech.* 42, 183 (1975).

[79] L. B. FREUND and R. J. CLIFTON, On the uniqueness of plane elastodynamic solutions for running cracks, *Jour. Elasticity* 4, 293 (1974).

[80] N. I. MUSKHELISHVILI, Singular Integral Equations, Noordhoff Publishing Co., (1953).

[81] A. H. STROUD and D. H. SECREST, Gaussian Quadrature Formulas, Prentice-Hall (1966).

APPENDICES

APPENDIX A

Baker's Solution: Part I

Baker [31] investigated a semi-infinite crack suddenly appearing in a uniformly stretched elastic medium at t = 0 and propagating at constant speed. A fixed coordinate system is introduced in such a way that the crack is defined by the negative x-axis and the crack propagates along the positive x-axis. The normal displacement of the upper crack surface in terms of the normalized variables defined in 2.1 is given by

$$v(x,0,t) = \sigma At + H\left(\frac{x}{t} + 1\right) \frac{\sigma A t}{4\pi F_+^*(-\infty)} \times$$

$$\int_{-\frac{1}{A}}^{\frac{x}{At}} F_+^*(u) \left(\frac{x}{At} - u\right) \frac{u^2(1-u)^{1/2}(1-A^2u^2)^{1/2}}{(\delta-u)^{3/2}} \times$$

$$\left[\begin{array}{ll} \dfrac{(1-u^2/2)^3}{(1-u^2/2)^4 - (1-u^2)(1-A^2u^2)}, & -\dfrac{1}{A} \le u < -1 \\ \dfrac{1}{(1-u^2/2)^4 - (1-u^2)^{1/2}(1-A^2u^2)^{1/2}}, & -1 < u < \delta \end{array}\right] du , \qquad (A.1)$$

where $x < ct$, σ is the uniform tensile stress applied to the medium, $\delta = c/A$, and

$$F_+^*(u) = \frac{(1-\delta)(P-u)}{(P-\delta)(1-u)} \exp\left\{\frac{1}{\pi}\int_A^1 \tan^{-1}\right.$$

$$\left[\frac{(y^2-1/2)^2}{y^2(1-y^2)^{1/2}(y^2-A^2)^{1/2}}\right] \frac{dy}{y(1-\delta y)+(1-\delta y)^2/(\delta-u)} \Bigg\} ,$$

where $P = C_R/A$.

Differentiation of (A.1) with respect to x yields

$$v_{,x}(x,0,t) =$$

$$\frac{\sigma}{4\pi F_+^*(-\infty)} \int_{-\frac{1}{A}}^{\frac{x}{At}} F_+^*(u) \frac{u^2(1-u)^{1/2}(1-A^2u^2)^{1/2}}{(\delta-u)^{3/2}} \times$$

$$\left[\begin{array}{ll} \dfrac{(1-u^2/2)^3}{(1-u^2/2)^4 - (1-u^2)(1-A^2u^2)} , & -\dfrac{1}{A} \le u < -1 \\ \dfrac{1}{(1-u^2/2)^2 - (1-u^2)^{1/2}(1-A^2u^2)^{1/2}} , & -1 < u < \delta \end{array}\right] du . \qquad \text{(A.2)}$$

If $x > -C_R t$, the bottom term in the bracket must be evaluated in the sense of the Cauchy principal value, since

$$\frac{1}{(1-u^2/2)^2 - (1-u^2)^{1/2}(1-A^2u^2)^{1/2}} =$$

$$\frac{16\,[(1-u^2/2)^2 - (1-u^2)^{1/2}(1-A^2u^2)^{1/2}]}{u^2(u+P)(u-P)[u^4+(-8+P^2)u^2+(24-16A^2-8P^2+P^4)]} .$$

Clearly, if x goes to $-C_R t^-$ or $-C_R t^+$, $v_{,x}(x,0,t)$ goes to infinity logarithmically. We can also observe from (A.2) that $v_{,x}(x,0,t)$ is continuous at the dilatational and shear wave fronts, that is, at $x = -t$ and $x = -At$, respectively.

APPENDIX B

Baker's Solution: Part II

Using the polar coordinate system shown in Figure 1, t_{yy} for Baker's problem (see Appendix A) for large values of t/r is given by the following asymptotic form:

$$t_{yy} \sim \frac{\sigma C_1 2^{1/2}}{\pi F_+(0)} \frac{1-\delta^2/2}{(1+\delta)^{1/2}} \left(\frac{tA}{r}\right)^{1/2} \left\{ - \frac{1-\delta^2/2}{(1-c^2)^{1/2}} \frac{[1+\cos\theta/d_1]^{1/2}}{d_1^{1/2}} + \frac{(1-\delta^2)^{1/2}}{(1-\delta^2/2)} \frac{[1+\cos\theta/d_2]^{1/2}}{d_2^{1/2}} \right\} , \qquad (B.1)$$

where

$$C_1 = \frac{(1-c^2)^{1/2}(1-\delta^2)^{1/2}}{(1-c^2)^{1/2}(1-\delta^2)^{1/2}-(1-\delta^2/2)^2} ,$$

$$d_1 = (1-c^2\sin^2\theta)^{1/2} ,$$

$$d_2 = (1-\delta^2\sin^2\theta)^{1/2} ,$$

$$F_+(0) = \frac{A-c}{P-c} \exp \left\{ \frac{1}{\pi} \int_{\frac{1}{1-c}}^{\frac{1}{A-c}} \frac{1}{w} \times \tan^{-1} \frac{\left[w^2 - \frac{(1+cw)^2}{2A^2}\right]^{1/2}}{w^2[w^2-(1+cw)^2]^{1/2} \left[\frac{(1+cw)^2}{A^2} - w^2\right]^{1/2}} dw \right\} ,$$

and σ, δ and P are defined as in Appendix A.

For $\theta = 0$, (B.1) reduces to

$$t_{yy} \sim \frac{2\sigma}{F_+(0)} (A-c)^{1/2}(t/r)^{1/2} . \qquad (B.2)$$

K_{ID} for this problem is obtained from (2.4.1) and (B2). In order to obtain K^*_{ID} for comparison with the results of this investigation, we divide K^*_{ID} by $K_{IS} = \sigma[\pi(1+ct)]^{1/2}$ and obtain

$$K^*_{ID} = k(A,c) \sqrt{t/(1+ct)} ,$$

where

$$k(A,c) = \frac{2\ 2^{1/2}}{\pi F_+(0)} (A-c)^{1/2} .$$

For $A = 0.542$ an evaluation of $F_+(0)$ by application of the Gauss quadrature formula (2.5.11) yields the following numerical values of $k(A,c)$:

c/A	k(A,c)
0.0	0.580
0.2	0.503
0.4	0.414
0.6	0.306
0.8	0.157

APPENDIX C

Cauchy Integrals Near Ends of the Line of Integration

The results stated in this appendix were obtained by N. I. Muskhelishvili [80]. The numbers of equations are the same as those in the reference.

Let L = ab be a smooth arc and let $\varphi(t)$ be a function, given on L, satisfying the following conditions:

a) On any closed interval $a'b'$ of the arc ab, not including the ends a, b, the function $\varphi(t)$ satisfies the $H(\mu)$ condition

$$|\varphi(t_2) - \varphi(t_1)| \leq A\,|t_2 - t_1|^{\mu}, \qquad (29.1)$$

where A does not depend on the position of t_1 and t_2 in the interval $a'b'$, but it may depend on the choice of a', b' (in fact, it may increase without limit when $a' \to a$ or $b' \to b$).

b) Near the ends a, b the function $\varphi(t)$ is the form

$$\varphi(t) = \frac{\varphi^*(t)}{(t-c)^{\gamma}}\,, \quad \gamma = \alpha + i\beta\,, \quad 0 \leq \alpha < 1\,, \qquad (29.2)$$

where c is either of the ends a, b, α and β are real constants and $\varphi^*(t)$ satisfies the H condition near and at c. In (29.2), $(t-c)^{\gamma}$ is any definite branch which

varies continuously on L. Further, note that for $\alpha > 0$ the condition (29.2) gives

$$\varphi(t) = \frac{\varphi^{**}(t)}{|t-c|^{\alpha}} , \tag{29.2a}$$

where $\varphi^{**}(t)$ is a bounded function such that $|t-c|^{\alpha}\varphi^{**}(t)$ satisfies the H condition for any $\epsilon > 0$ and vanishes for $t = c$. In fact,

$$\varphi^{**}(t) = \varphi^{*}(t)e^{-ia\vartheta}(t-c)^{-i\beta} ,$$

where $\vartheta = \arg (t-c)$; the proposition then follows by (7.3a) and (7.6), which are

$$\psi(t) = |t-t_0|^{\epsilon}\, e^{\alpha\vartheta},\ 0 < e \leq 1, \tag{7.3a}$$

where α is any constant.

$$\psi(t) = |t-t_0|^{\epsilon}\, [t-t_0]^{i\nu} \tag{7.6}$$

where ν is any real constant.

Next examine

$$\Phi(z) = \frac{1}{2\pi i}\int_{L} \frac{\varphi(t)\ dt}{t-z} . \tag{29.3}$$

Under the assumed conditions for the point z, which is near c but not on L, $\Phi(z)$ is of the form:

1) If $\gamma = 0$ [i.e, $\varphi^{*}(t) = \varphi(t)$],

$$\Phi(z) = \pm \frac{\varphi(c)}{2\pi i} \log \frac{1}{z-c} + \Phi_0(z) , \tag{29.4}$$

where the upper sign is taken for c = a, the lower for c = b. By $\log [1/(z-c)] = -\log(z-c)$ is to be understood any branch, one-valued near c in the plane cut

along L; $\Phi_0(z)$ is a bounded function tending to a definite limit when $z \to c$ along any path.

2) If $\gamma = \alpha + i\beta \neq 0$,

$$\Phi(z) = \pm \frac{e^{\pm\gamma\pi i}}{2i\sin\gamma\pi} \frac{\varphi^*(c)}{(z-c)^\gamma} + \Phi_0(z) , \qquad (29.5)$$

where the signs are chosen as in 1), $(z-c)^\gamma$ is any branch, one-valued near c in the planecut along L and taking the value $(t-c)^\gamma$ on the left side of L, and $\Phi_0(z)$ has the following properties: if $\alpha = 0$, it is bounded and tends to a definite limit when $z \to c$; if $\alpha > 0$,

$$|\Phi_0(z)| < \frac{C}{|z-c|^{\alpha_0}} , \qquad (29.6)$$

where C and α_0 are real constants such that $\alpha_0 < \alpha$.